

Development of a PPAR α/δ Agonist Drug for the Treatment of Postoperative Atrial Fibrillation

EPFL

BIO-494: Scientific Project Design in Drug Discovery

Supervisors:

Johan Auwerx
Giacomo Von Alvensleben
Adrien Faure

Authors:

Elisa Cabos, Charlotte Coulon, Claire Damery, Maïka Nogarotto, Burcu Özer, Alexandra-Elena Preda, Victoire Ringler, Kenza Rhachi, Bettina Weber and Danja Zengaffinen

Content

1. Abstract.....	2
2. Introduction	2
2.1 POAF Occurrence and Underlying Mechanisms	2
2.2 PPAR as a Target Treatment for Mitochondrial Dysfunction	2
2.3 Drug Chosen to Control the Target.....	3
2.4 Target Product Profile	3
2.5. Drug Development Process Overview.....	4
3. In Silico Screening.....	5
3.1 PPAR Structures.....	6
3.2 Ligands Library Design.....	6
3.3 Docking.....	8
3.4 Future Developments	9
4. In Vitro Screening and Assays	9
4.1 In Vitro Screening	9
4.3 Primary Assays	11
4.4 Secondary Assays	12
5. In Vivo Validation	13
5.1 Animal Selection.....	13
5.2 Pharmacokinetics (PK).....	14
5.3 Pharmacodynamics (PD)	15
5.4 Primary Studies for Efficacy.....	16
5.5 Chronic Studies	17
5.6 Secondary Studies in Vivo: Toxicology.....	17
6. Clinical Trials	17
6.1 Phase I	17
6.2 Phase II	19
6.3 Phase III	21
6.4 Phase IV.....	21
7. Business Plan.....	21
8. Conclusion.....	22
9. Bibliography	23
10. Supplementary Material	30

1. Abstract

Post-operative atrial fibrillation (POAF) is a common complication following cardiac and non-cardiac thoracic surgeries, with significant associated risks, increased morbidity and mortality. This condition has been linked to mitochondrial dysfunctionality which can disrupt fatty acid oxidation, contributing to metabolic imbalances that predispose individuals to atrial fibrillation [1]. Despite measures such as β -blockers, which are used for lowering blood pressure and heart rate, POAF still occurs in 20-40% of cardiac surgical procedures and 10-20% of non-cardiac thoracic procedures [2]. Addressing this lack of efficacious treatment options, we explore a novel approach to preventing POAF by targeting peroxisome proliferator-activated receptors (PPARs), specifically PPAR α and PPAR δ . These receptors are crucial in fatty acid metabolism within the mitochondria, particularly in the β -oxidation of the long-chain fatty acid acetyl-coenzyme A in the mitochondrial matrix [1]. Our drug, Rythmiar, aims at reducing POAF occurrence by at least 70%.

Development begins with in silico screening, which uses computational methods to find promising compounds by integrating both structure- and ligand-based virtual screenings. Subsequent in vitro assays will be used to determine the specificity, toxicity, binding affinity and activation of fatty acid oxidation pathways. In vivo validations in selected animal models, including rodents, Göttingen pigs and German Landrace pigs will provide information on pharmacokinetics, pharmacodynamics, and long-term effects, which are all crucial for assessing safety and efficacy. Finally, clinical trials will have the primary outcome of reducing POAF occurrence by 70% in patients over 40 undergoing coronary artery bypass graft surgery through pre- and post-operative continuous intravenous infusion of the drug. In the future, Rythmiar's application could be extended to other surgery complications and conditions like acute kidney injury (AKI) and chronic atrial fibrillation (CAF), for which an oral formulation of the drug would be developed. This would further bolster the projections for the drug's market potential and financial viability.

2. Introduction

2.1 POAF Occurrence and Underlying Mechanisms

Post-operative atrial fibrillation (POAF) is a surgical complication that arises upon 20-40% of cardiac surgical procedures and 10-20% of non-cardiac thoracic procedures [2]. The occurrence of POAF is most often episodic, with a peak around 2 to 4 days postoperatively, and usually ends with a spontaneous return to a healthy sinus rhythm. In addition to extending hospital stays and thus increasing costs, POAF causes hemodynamic instability, increased risk of stroke, increased short-term and long-term morbidity and mortality, an eight-fold increase in the risk of subsequent atrial fibrillation (AF), and a higher rate of cardiovascular death [2].

Due to the complexity of the underlying mechanisms and the interactions of predisposing factors, the causes of POAF remain unclear. However, cardiac ischemia, inflammation, sympathetic activation, obesity, age, hypertension, diabetes, dyslipidemia, tobacco use, and cardiac diseases have all been linked to higher rates of POAF [3]. Due to the difficulty of establishing causal links between the predisposing factors and the occurrence of POAF, current treatments mainly consist of prophylaxis and control. The best-established prevention is based on the prophylactic administration of different types of β -blockers to diminish myocardial oxygen requirements and overall ischemic events [4]. If POAF does occur, the usual treatment is rate control, rhythm control being reserved for patients who develop hemodynamic instability [3].

2.2 PPAR as a Target Treatment for Mitochondrial Dysfunction

Research suggests that fatty acid oxidation (FAO) in the mitochondria plays an important role in cardiac metabolism, since fatty acids (FAs) are the primary energy source of the myocardium, especially when confronted with the metabolic demands and oxygen fluctuations that accompany surgery and post-operative period [5], [6].

Mitochondrial FAO involves the uptake and activation of FAs in the cytoplasm, their transport into the mitochondria, and subsequent β -oxidation in the mitochondrial matrix, leading to

adenosine triphosphate (ATP) production via the Krebs cycle. The disruption in mitochondrial FAO typically occurs during the β -oxidation step in the mitochondrial matrix. In this phase, impaired oxidation of FAs can result in inadequate ATP production, affecting the energy balance within heart cells and potentially contributing to altered electrical and mechanical functioning in the heart, which is a key factor in the onset of AF [7].

Mitochondrial FAO is an inherently efficient pathway compared to glycolysis when oxygen levels are reduced such as during cardiac surgery. Maintaining it would thus provide continuous, adequate ATP production and ensure mitochondrial function in order to reduce stress that could generate cardiac arrhythmias [8]. Furthermore, a strong connection has been observed between FAO and anti-inflammatory effects, particularly through the modulation of macrophage activity. This anti-inflammatory response could be beneficial in preventing postoperative complications, including AF [9].

For these reasons, we investigated peroxisome proliferator-activated receptors (PPARs), a family of nuclear receptor proteins that play a crucial role in regulating many processes including mitochondrial FA metabolism, occurring in the mitochondrial matrix. The three existing isoforms, PPAR α , PPAR δ and PPAR γ function as transcription factors that control the expression of genes involved in FAO. Their activation could reduce POAF occurrence. We will mainly focus on PPAR α and PPAR δ since they are more specific to the heart than PPAR γ [10].

2.3 Drug Chosen to Control the Target

As mentioned, the molecular targets of our drug Rythmiar will be PPAR α and PPAR δ . When bound to FA ligands, these nuclear receptors are translocated to the nucleus where they bind to the nuclear receptor response element (NRRE) with their partners and coactivators RXR and PGC1. The latter attract further molecules, forming a complex that promotes the transcription and RNA splicing of genes involved in FAO, specifically myocardial FAO for PPAR δ , thus regulating the energy metabolism in cardiomyocytes [11], [12]. We aim at developing a molecule that binds and stabilizes PPARs' complexes to stimulate this mechanism.

2.4 Target Product Profile

The intravenous route for our product is chosen for its rapid onset, precise dosing, and reliability, particularly beneficial in a hospital setting for close monitoring and immediate response. It's also suitable for patients with absorption issues or those unable to take oral medications [2]. Additionally, continuous infusion before and after surgery ensures steady medication delivery and optimal drug levels during critical periods [13]. The expansion to acute kidney injury (AKI) and chronic atrial fibrillation (CAF) is possible because both these diseases are linked to PPAR α and PPAR δ agonist mediated mitochondrial FAO [14], [15] (See **Table 2.1** for a description of the target product profile).

Parameter	Essential Profile	Extended Profile
Indications	Post-operative, acute phase AF	Expansion to AKI and CAF
Patient Population	Patients 40+ years old, undergoing coronary artery graft bypass surgery	Expansion to other cardiac surgeries and all surgeries involving extracorporeal circulation and AKI, CAF
Therapeutic modality	Nuclear Receptor Ligand	
Efficacy	$\geq 70\%$ decrease in occurrence of AF within 7 days post-surgery. (Compared to the occurrence of AF post-surgery without medical intervention)	TBD
Safety	$\leq 20\%$ incidence of adverse side effects such as dizziness, tiredness, abdominal discomfort, epigastric pain, nausea, and vomiting and no serious adverse side effects (i.e., death)	

Dosing and Administration	Continuous infusion pre- and post-operatively. Start of treatment: one day pre-operatively Duration of treatment: six days post-surgery (subject to adjustments from pre-clinical trial results in animal models)	Oral, once-daily administration
Mechanism of Action	Activation of PPAR α and δ nuclear receptors resulting in increased mitochondrial FA metabolism in the heart	

Table 2.1: Target product profile for Rythmiar. Abbreviations: AF = Atrial Fibrillation; AKI = acute kidney injury; CAF = chronic atrial fibrillation; TBD = to be defined

2.5. Drug Development Process Overview

An overview of the drug development process can be seen in **Figures 2.1** and **2.2**.

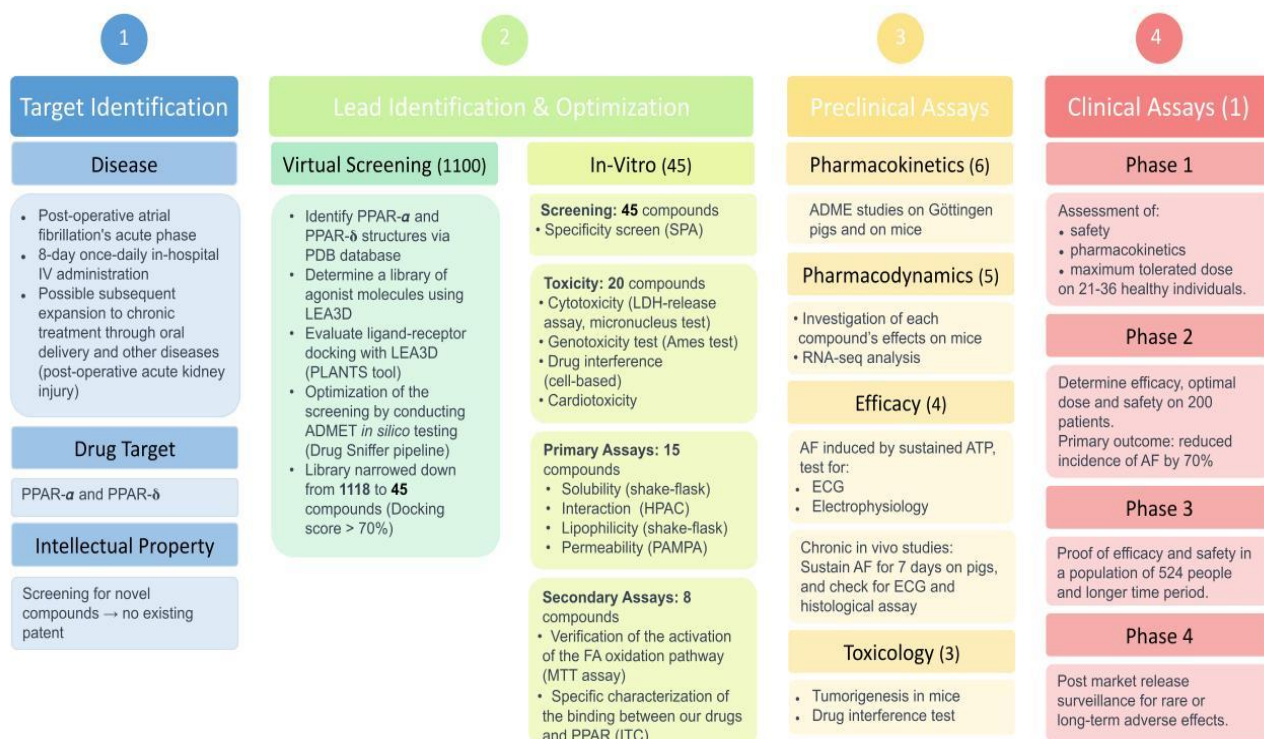


Figure 2.1: Overview of drug development.

Abbreviations: IV = Intravenous; PPAR- α (δ) = peroxisome proliferator-activated receptor-alpha (delta); (#) = Number of compounds assessed in the corresponding step; LEA3D = Computer-Aided Ligand Design and screening software; PLANTS = Protein-Ligand ANTSsystem; ADME(T) = absorption distribution metabolism excretion (Toxicity); SPA = Scintillation Proximity Assay; LDH = Lactate Dehydrogenase; HPAC = High-Performance Affinity Chromatography; PAMPA = Parallel Artificial Membrane Permeability Assay; FA = Fatty Acid; ITC = Isothermal Titration Calorimetry; AF = Atrial Fibrillation; ATP = Atrial Tachypacing; ECG = Electrocardiogram.

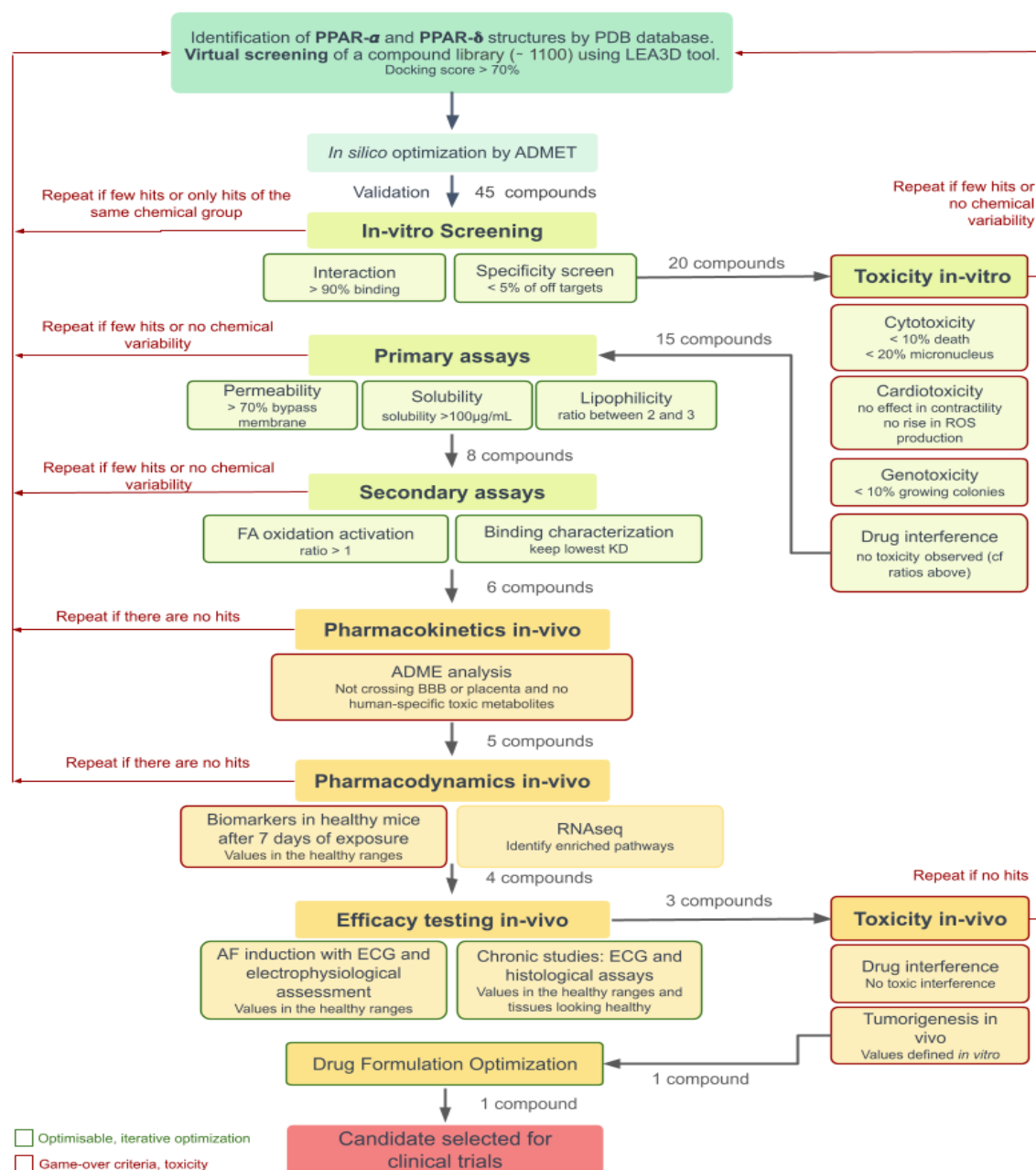


Figure 2.2: Flow chart of drug development.

Abbreviations: PPAR- α (δ) = peroxisome proliferator-activated receptor- α (δ); PDB = Protein Data Bank; LEA3D = Computer-Aided Ligand Design and screening software; ADME(T) = absorption distribution metabolism excretion (Toxicity); FA = Fatty Acid; KD = Dissociation rate; BBB = Blood Brain Barrier; AF = Atrial Fibrillation; ECG = Electrocardiogram; ROS= Reactive Oxygen Species.

3. In Silico Screening

Over the last few years, computational (*in silico*) methods have gained importance and have been used for pharmacological structure predictions and testing in drug discovery. Computer aided drug discovery (CADD) methods are often utilized in conjunction with *in vitro* data, serving a dual purpose of building and assessing predictive models. These models identify new molecules that exhibit a specific binding affinity towards a particular target [16]. The initial step for CADD is screening available molecular databases. This involves two approaches: structure-based virtual screening (SBVS) which uses a target protein structure to predict its binding to ligands, and ligand-based virtual screening (LBVS) which uses a reference ligand to predict structurally similar compounds to the reference [17].

To generate a library of potential compounds that can bind and activate PPAR α and PPAR δ , we combined both approaches by first applying LBVS to enrich our database of candidate

ligands and then testing these candidates' binding likelihood to our targets through SBVS. Our main goal is to narrow down the candidate compounds, which are going to be further tested and validated *in vitro*, to save time, money and materials. In addition, we aim to investigate whether there are any dual agonist ligands that bind to both PPAR α and PPAR δ to make the ligands potentially more suitable for broader applications of our drug.

3.1 PPAR Structures

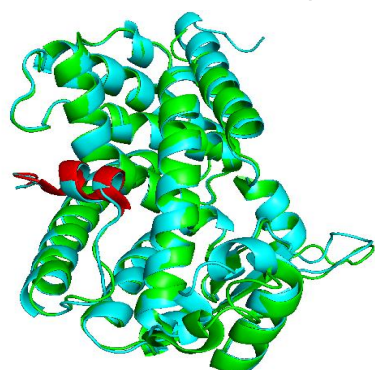
For SBVS, to identify the available PPAR α and PPAR δ molecular structures, we used the UNIPROT Knowledgebase [18], a database of functional information on proteins. From there, we found the experimental structures that are deposited in Protein Data Bank (PDB) [19], a database for 3D structures of large biomolecules. Among the structures that were characterized with different experimental methods, we chose 1K7L (PPAR α) [20] and 3TKM (PPAR δ) [21] because of their large protein sequence coverage and high resolution. However, all structures that we found contained a ligand bound to the protein (GW409544 for PPAR α and GW0742 for PPAR δ), introducing a conformational change. We therefore also used AlphaFold [22], [23] for structures predicted with artificial intelligence.

To predict the potential binding sites of the target structures, we used an online tool (COACH) based on structural and sequence alignments [24], [25]. Thus, information such as consensus binding residues (several residues creating a binding pocket), center coordinates of the binding pocket and C-score (confidence score of the prediction) are generated for potential binding sites. An example output that COACH generates can be seen for PPAR α in **Figure 3.1** where the predictions are ranked according to the C-score. We used the binding site prediction with the highest C-score for each of the structures (PDB and AlphaFold) for the docking simulations. Other binding site predictions will also be tested in the future.

Rank	C-score	Cluster size	PDB Hit	Lig Name	Download Complex	Consensus Binding Residues
1	0.92	1358	4iwwA	1GJ	Rep. , Mult	72,75,76,79,82,113,116,120,123,150,153,154,157,239,242,243,246,259
2	0.84	967	4iu7B	PEPTIDE	Rep. , Mult	87,91,101,104,105,108,109,257,258,261,262
3	0.43	452	2q59B	240	Rep. , Mult	72,75,76,78,79,82,86,116,117,119,120,123,129,131,138,153,154,157,239,243

Figure 3.1: Top 3 binding site predictions of PPAR α PDB structure (1K7L) in COACH.

To observe the conformational differences between PDB and AlphaFold structures, we performed structural alignment and observed a root mean square deviation of 0.540 for PPAR α and 0.491 for PPAR δ . These low values demonstrate that there were only slight differences between the PDB and AlphaFold structures as shown in **Figure 3.2** for PPAR α . In their inactive conformations, PPARs include the helix 12 (Activation Function-2) structure folding over the binding pocket. When an agonist ligand binds to it, helix 12 locates itself in an open conformation so that coactivator proteins can bind to PPAR to promote transcription [26], [27].



In **Figure 3.2**, helix 12 adapts a similar conformation for PDB and AlphaFold structures showing that they are both in active conformations. PPAR δ , which is not shown here, also demonstrates a similar conformation and alignment in helix 12 for both PDB and AlphaFold structures.

Figure 3.2: Structural alignment of PPAR α PDB structure in active conformation (in green) and AlphaFold structure (in blue) created using PyMOL [28]. Helix 12 of the PDB structure is shown in red.

3.2 Ligands Library Design

After exploring the structures of PPAR α and PPAR δ , we proceeded to identify candidate ligands through LBVS and establish a molecular library. Our small molecules will be agonists as they bind and activate either one of the PPAR types or both at once.

First, by literature search [11], we identified known natural and synthetic agonist ligands. Natural ligands (Supplementary **Table S1**) consist mainly of Omega-3 polyunsaturated FAs. Being known to bind their receptors with high affinity (nanomolar scale) and activate them [29], the aim of considering these natural compounds in the future will be to validate the structure of the designed new ligands. On the other hand, synthetic ligands such as fibrates, GW501516 and Elafibranor, which is a dual agonist for PPAR α and PPAR δ , were used to collect multiple reference structures (Supplementary **Tables S2** and **S3**) from the PDB database [19]. These reference molecules were then used to determine *de novo* ligands.

For our product, we used the online LEA3D server to come up with *de novo* ligands using a similarity percentage score [30]. LEA3D is a computer-aided drug design web server that depends on fragment molecules. It has a fast and comprehensive system that combines different tools for SBVS and LBVS. One tool it offers for LBVS is the *de novo* drug design which facilitates the creation of new compounds by optimizing a user-specified scoring function [31]. The newly generated molecules are created through modifications on reference molecules by mutation (suppression, addition, replacement or permutation of a fragment) or crossover (recombination of pre-existing fragments) operators [32]. Each submission runs for a maximum of 50 generations, with the top candidate (best score in percentage) of each generation represented as an output [31].

Two methods were used to generate candidate compound libraries through *de novo* drug design: one with and one without specific constraints which incorporate some molecular properties to refine the libraries.

3.2.1 Method without Constraints

Through SenSaaS (SENSitive Surface as a Shape), a tool within LEA3D, we estimated molecular shape similarity to uploaded reference molecules using flexible molecule alignment. In this process, each run evaluated 2040 new molecules across several generations (up to a maximum of 50), and the best molecule from each generation was presented as a result. The purpose of considering a method without constraints was to have a large number of potential new ligands that will be optimized in the future by making them more drug-like thus having favorable ADME (absorption, distribution, metabolism and excretion) characteristics.

3.2.2 Method with Constraints

Using LEA3D we also added constraints by using specific ranges for several molecular properties along with a weight equal to one in the final score for most of these properties (Supplementary **Table S4**). Having these ranges allowed us to ensure that the new ligands possess drug-like properties. Moreover, the equal weighting of the final score ensured that all the molecular features had the same level of influence on the results. We mainly based our choice on Lipinski's rule of five and other relevant properties for our drug. In fact, this rule of five is often involved in drug discovery by suggesting properties based on empirical observations [33]. The assessment of whether a molecule potentially has the chemical and physical properties to be orally bioavailable was based on four specific properties: no more than five hydrogen bond donors, no more than 10 hydrogen bond acceptors, molecular mass less than 500 Da, and a partition coefficient (MolLogP) not greater than five. According to Lipinski's rule, an orally active drug can have no more than one violation of these conditions [33]. Having the goal in mind to expand our drug from IV to oral administration, those factors were relevant for the development of our product. Furthermore, when constraints are used, LEA3D has the option of conducting *de novo* drug design both with and without reference structures and both options were explored. Since this method uses restrictions to generate new ligands, the resulting number of candidates was smaller compared to the method without constraints.

Overall, using the methods described in Section 3.2.1 and 3.2.2, a library of candidate compounds was generated for each type of synthetic ligand. The total number of these compounds was 1118.

3.3 Docking

To screen the compound libraries that were generated in Section 3.2 and test their binding abilities with our targets (PPAR α and PPAR δ), we performed molecular docking. Apart from its *de novo* drug design tool, LEA3D also performs docking using PLANTS (Protein-Ligand ANT System) [34]. PLANTS uses an algorithm that treats the ligand as flexible whereas keeping the protein partially flexible on its side chains to optimize a minimum energy conformation.

Since PLANTS does not change the backbone conformation of the proteins, it may not be able to optimize the inactive conformation of the target. Therefore, using the active conformation of PPAR as an input in docking is more promising for testing the binding capabilities of ligands. For this reason, we decided to use only the PDB structures as they represent the active conformation more accurately than the AlphaFold predictions.

As input parameters for docking, we used the center coordinates of the binding pocket predicted by COACH and a default binding site radius of 10Å, which was observed to cover all the binding residues in PyMOL [28]. We performed docking for each compound type separately and evaluated them based on their docking scores. The docking score is provided by PLANTS and it assesses the steric complementarity of the protein-ligand complex [34]. We selected a docking score of 70% as a threshold and selected the ligands that have a higher score as candidates. As a result, we ended up with 62 ligands for PPAR α and 70 ligands for PPAR δ . Among these ligands, 45 ligands reached the threshold for both PPARs and therefore represent the dual-agonist ligands that will further be evaluated with the *in vitro* screening and testing. Consequently, the library of candidate compounds shrinks from 1118 to a total of 45 dual-agonist ligands.

The best candidates of each compound type for PPAR α are shown in **Table 3.1**, where they are classified depending on the usage of constraints. Similar score rankings and classifications were also conducted for PPAR δ . The simulations performed in Section 3.2.2 without any reference structure were not included as their scores were below 70%. In addition, the dual agonist ligands with the highest scores are shown in Supplementary **Table S5**. To be able to examine the binding of the best dual agonist ligand, its protein-depicted in **Figure 3.3** where similar binding pockets can be observed for PPAR α and PPAR δ .

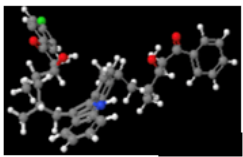
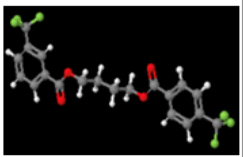
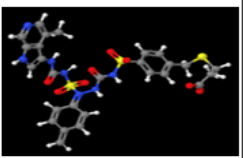
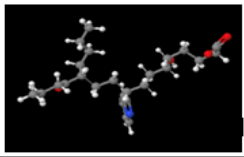

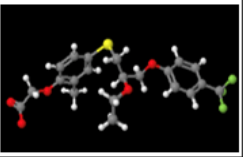
Synthetic Compounds	Fibrates		GW501516		Elafibranor	
	Score	Ball-and-Stick Model	Score	Ball-and-Stick Model	Score	Ball-and-Stick Model
Without Constraints	98.80%		75.62%		82.30%	
With Constraints	76.85%		71.60%		70.32%	

Table 3.1: Ligands with the highest docking scores with PPAR α for each synthetic compound type

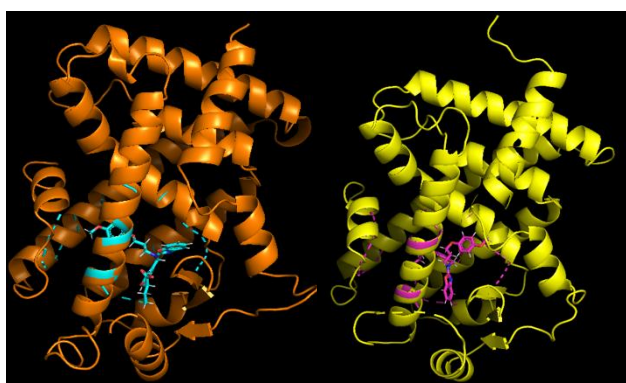


Figure 3.3: Binding of the best dual agonist ligand (with constraints) for PPAR α (in orange) and PPAR δ (in yellow). The dashed lines represent the binding site sphere and the ligand, which adapts different conformations for both, is shown at the center of them (in cyan for PPAR α and in magenta for PPAR δ).

3.4 Future Developments

Same screening steps will be repeated with thousands of compounds in the future, as have been described with the first 1118 of them in this report. This way, a higher docking score threshold for selection will be used. Then, once the library of candidate compounds is narrowed down with docking, lead optimization will be performed on the selected chemical structures using pharmacophore modeling tools such as Phase to make them gain drug-like properties [35], [36]. Additionally, we can also use the Drug Sniffer tool [37] which performs all the steps from *de novo* ligand design to molecular docking as well as ADMET (Absorption, Distribution, Metabolism, Excretion and Toxicity) prediction [38]. For ADMET prediction, it uses several molecular fingerprint-based predictive models that evaluate multiple properties such as HERG cardiotoxicity, toxic myopathy, and mitochondrial toxicity [39]. These properties are particularly interesting since they will guide the toxicity tests that will be performed *in vitro*. Furthermore, as the docking simulations (LEA3D and Drug Sniffer) do not consider the backbone flexibility of the protein, we will conduct molecular dynamics simulations using CHARMM-GUI [40] to simulate the conformational flexibility of the protein-ligand complex and dynamically observe their binding. Finally, both PPAR α and PPAR δ can be associated with different mutations that might cause conformational changes [37], [38]. Therefore, the common mutations will be identified from the literature and checked to determine if they correspond to the binding sites and affect the binding of the candidate ligands.

4. In Vitro Screening and Assays

4.1 In Vitro Screening

After the virtual screening, a set of 45 potential candidates will undergo *in vitro* screening in order to ensure a specific interaction of our drug with our targets PPAR α and PPAR δ and validate the results from the *in silico* screenings.

4.1.1 Screen for the interaction between PPAR and our Candidate Drugs

In order to further select molecules that bind with high affinity to PPARs, high-performance affinity chromatography (HPAC) will be used [41]. HPAC is useful in early drug discovery as it gives information about the amount of binding (%) after a single injection [41]. The percentage of binding of the molecule is obtained from its retention factor k at equilibrium:

$$\% \text{ binding} = \frac{k}{k+1} [42].$$

This procedure requires only a small amount of protein, and at the same time enables a large number of experiments, since the same protein preparation can be reused multiple times [41]. It relies on the immobilization of PPARs on a support. It is of utmost importance to not disturb their natural conformation when binding to the column, and to leave the binding site accessible to the drug. To ensure a proper immobilization, methods such as biotin-(strept)avidin interaction can be used. By genetic engineering, PPARs can be fused to biotin [43] at their N-terminal, as it interferes less with the 3D structure [11]. Then, the biotinylated protein can be immobilized on avidin, streptavidin or monomeric avidin supports [43]. A solution containing the molecules of interest is injected into the column and the drugs targeting PPARs with high affinity elute later than the ones with lower or no affinity [41]. We will also test whether the drug candidates could bind to the common mutations of PPAR as mentioned in the *in silico* section. A candidate is kept if it has a binding of at least 90%.

4.1.2 Specificity Screen

The specificity of our candidate drugs can be investigated using a technique called ligand-binding assay (LBA), enabling us to determine possible off-targets. Different proteins are tested for their interaction with our candidate drugs, including proteins conformationally similar to PPARs and proteins targeted by FDA approved drugs: proteins that circulate in the blood (such as thrombin, Xa factor), and some proteins that reside in the cardiomyocytes (beta adrenoceptors, potassium channels). This ligand-binding assay is implemented in a 96-well plate, with each well corresponding to a protein-ligand combination. The interaction can be measured by scintillation proximity assay (SPA), a labeling strategy not disrupting the affinity of the binding [44]. The protein is immobilized on a solid surface, and the ligand is labeled with a

radioactive isotope, ^{125}I [44]. Light is emitted as a result of energy transfer from the radioactive decay of the ligand to the bead (scintillant) attached to the protein, when they are in close proximity [44]. The principle of this technique can be seen in **Figure 4.1**. We will quantify the emitted light by measuring the absorbance at a certain wavelength of the solution. The negative control is established by measuring the absorbance without adding any ligand and the positive control is done by adding a ligand for which we know that it binds with high affinity to the protein of interest (for example, common drugs that bind to the protein). We keep a drug candidate if it has less than 5% of binding to the tested proteins.

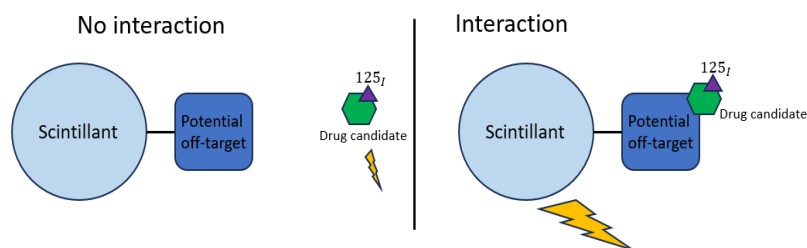


Figure 4.1: Scintillation proximity assay (SPA) principle.

4.2 Toxicity Assays

After the specificity screen, we are left with an estimate of 20 potential drugs, which will pass through the toxicity assays.

4.2.1 Cytotoxicity

A molecule is defined as cytotoxic if it significantly interferes with cell morphology and physiology, causing cell death. Each tested compound will be added separately into a cell culture and incubated for a few hours. Then, the presence of dead cells that have lost their membrane integrity will be assessed by measuring released lactate dehydrogenase (LDH) activity [45] by a fluorogenic LDH-release assay [46] explained in **Figure 4.2**. An excess amount of lactate, NAD^+ , and resazurin is added into the cell mixture allowing the extracellular LDH to convert NAD^+ into NADH, a very powerful reducing agent that converts resazurin into a fluorogenic product (resorufin) in the presence of the diaphorase enzyme. Finally, the amount of resorufin, proportional to the released LDH quantity, can be measured using a plate reading fluorometer. All the compounds causing more than 10% of cellular death will be discarded. The selection of this strict threshold is dictated by the nature of our drug that will interfere with cardiomyocytes which are essential for the tissue homeostasis.

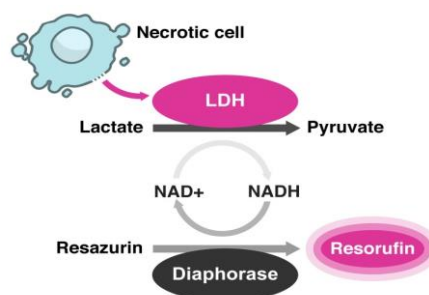


Figure 4.2: Schema of the fluorogenic LDH-release assay. From Cytotoxicity Assays: In Vitro Methods to Measure Dead Cells [46].

A micronucleus test [47] will also be performed, as micronuclei are biomarkers of potential genotoxic effects generated from mitosis malfunctioning upon exposure with the tested molecule. This assay consists of determining the micronucleus formation frequency in a treated cell culture. A candidate drug showing micronucleus formation in more than 30% of cell divisions will not be selected to undergo further secondary assays.

Toxicity testing will be performed on multiple cell types, listed in **Table 4.1**. Knowing that our drug will be metabolized by the liver, these tests will be repeated on hepatocytes. Keratinocytes will also be tested as our drug could have skin contact with the patient or doctors during the IV injection procedure. Other cell types could be further tested depending on the *in vivo* distribution results.

Cell type	Cell line	Application
Cardiomyocyte	AC16 Human Cardiomyocyte[48]	Study cardiac function and gene expression during normal and pathological conditions
Keratinocyte	HaCaT	High capacity to differentiate and proliferate
Hepatocyte	HepaRG [49]	Increased metabolic activity to give more predictive value for toxicity assays

Table 4.1: The different cell types and cell lines that would be used in the cytotoxicity screen.

4.2.2 Genotoxicity

Potential mutagenic properties of the candidate molecules will be determined by the Ames test [50], which uses mutated strains of *Salmonella* bacteria. These strains carry mutations in the

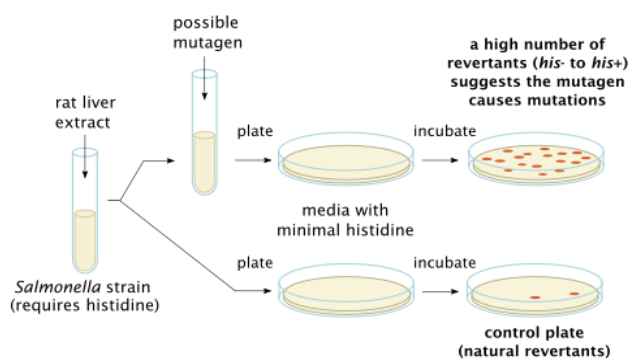


Figure 4.3: Schema of the Ames test [51].

genes involved in the histidine synthesis, preventing them from producing it. The test quantifies the capability of a given compound to induce mutations by exposing these strains to the compound and growing them on a histidine free-medium (See **Figure 4.3**). By counting the number of viable colonies that have regained the capability of synthesizing histidine, the mutagenic properties are quantified. The compounds presenting more than 10% growing colonies would not be further used since they are characterized as highly mutagenic.

4.2.3 Cardiotoxicity Tests

The introduction of synthetic substances in the heart can lead to cardiomyocyte dysfunction and damage. Knowing that the final drug will essentially target the heart, cardiotoxicity outcomes will be extensively tested in order to minimize potential heart issues caused by the drug injection. The *in vitro* cardiotoxicity will be evaluated on the AC16 Human Cardiomyocyte cell line.

Contractile Activity: After exposing the cardiomyocytes to a compound, the contractile activity can be microscopically determined and analyzed in order to compare their physiology before and after drug exposure. Since the contractile activity of cardiomyocytes is temperature dependent, the temperature of the microscope stage will be controlled. Each compound should not affect the contractile activity to any extent [48].

Intracellular Reactive Oxygen Species Production Assay: Nitroblue tetrazolium (NBT), an oxidative marker, is added to a cardiomyocyte culture previously exposed to the tested compound. NBT is oxidized by the reactive oxygen species (ROS), produced by the cardiomyocytes in the mitochondria, producing NBT-formazan which has a specific absorbance at 550nm. The concentration of the oxidized form of NBT can be measured spectrophotometrically and the ratio between NBT-formazan and initial NBT load will show the concentration of ROS produced by the tested cardiomyocytes. Tested molecules leading to higher ratios than in normal condition would not be selected because they increase ROS production in mitochondria, thus promoting AF [52].

4.2.4 Testing Drug Interference to Common AF Drugs

As drugs interfere with the metabolism of cells, it is of great importance to test whether our candidate drugs could potentially interfere with common approved drugs that could be taken in combination with ours and ensure the absence of negative effects. A cell-based approach will be implemented where our candidate drugs can be administered to cultures of cardiomyocytes, in addition to a panel of common AF drugs. This includes, among others, β -blockers (administered to control heart rate, like Betapace AF). Certain patients also receive anti-coagulation drugs that will be included in our assay (heparin, enoxaparin or dalteparin in combination with Coumadin or Aspirin (or both) in the acute conversion to sinus rhythm) [53]. Then, the different combinations of drugs are assessed for cytotoxicity, cardiotoxicity and genotoxicity of the *in vitro* assays as presented above in this section, and a candidate is kept if it passes their corresponding thresholds.

4.3 Primary Assays

The remaining candidates, expected around 15, will undergo a series of *in vitro* assays to select only the molecules with relevant physical properties. Although these important physical

properties have already been simulated during the virtual screening, the suggested *in vitro* assays will act as validation.

4.3.1 Solubility Screen

Considering that the final drug will be delivered by IV injection, solubility will play an important role and only highly soluble molecules will be selected for further and more in-depth screens. The shake-flask protocol [54] will be used. The compound of interest is dissolved in DMSO and linear serial dilutions are performed in an aqueous buffer until precipitate formation. Thanks to a membrane, the precipitates are filtered out and the fraction still in solution can be determined by UV or LC-MS (Liquid chromatography–mass spectrometry) using calibration curves. Only candidates with an aqueous solubility >100µg/mL will be kept in order to reduce the potential solubility-related issues that might be encountered during drug development. This test will be performed for different pH values in a range close to the human body's one in order to mimic as closely as possible the IV delivery condition.

4.3.2 Lipophilicity Screen

Since our drug targets a gene activator, it needs to easily bypass the nuclear membrane, meaning it should be sufficiently lipophilic to readily pass through the cell membranes but not so lipophilic to get stuck. One common way to determine the molecule lipophilicity consists of mixing a given compound quantity into a medium composed of an aqueous phase buffered with phosphate at pH 7.4 and an organic solvent. Then, the compound concentration in each phase is determined by UV spectrophotometry and, based on the shake-flask procedure [55], the ratio between the compound concentration in the organic phase and its concentration in the water phase provides a measure of lipophilicity. Only compounds with a ratio between 2 and 3 would be kept in order to remove highly and poorly lipophilic molecules.

4.3.3 Permeability Screen

The parallel artificial membrane permeability assay (PAMPA) [56] will be performed on a 96-wells plate setup to analyze simultaneously the purely passive diffusion of all the different compounds through an artificial cell membrane. Then, with LC-MS/MS, the molecules on both sides of the membrane are quantified to determine the molecule's permeability. Only compounds capable of bypassing the membrane for more than 70% of the initial amount will be selected. Several different types of artificial cell membranes are available, made from organic to inorganic material. Here we will use a polymeric organic synthetic membrane to mimic as closely as possible human cell membranes [57].

4.4 Secondary Assays

After the primary assays, we predict to have 8 compounds left that will undergo the secondary assays.

4.4.1 Verification of the Fatty Acid Oxidation Pathway Activation

The main purpose of our drug is to stimulate the FAO pathway in cardiomyocytes. We will verify the pathway activation with a succinate dehydrogenase MTT assay. The enzymatic reduction of 3-[4,5-dimethylthiazol-2-yl]-2,5-diphenyltetrazolium bromide (MTT) to MTT-formazan is catalyzed by mitochondrial succinate dehydrogenase, and is therefore dependent on the mitochondrial respiration, which mainly derives from the mitochondrial β -oxidation fatty acid pathway [52]. Hence, by measuring the concentration of MTT-formazan, it is possible to determine the level of activity of the pathway. MTT-formazan concentration is quantified thanks to a colorimetric reaction, from which the absorbance is measured at 570 nm.

A candidate is kept if the ratio $\frac{[MTT-formazan]_{with\ drug}}{[MTT-formazan]_{without\ drug}} > 1$.

4.4.2 Specific Characterization of the Binding between our Drugs and PPAR

To characterize binding mechanisms after assessing binding affinity with primary screening, we will perform isothermal titration calorimetry (ITC), with the advantage that the step of protein immobilization on a surface is absent. This method measures the heat uptake or release upon complex formation [37] and consists in the successive addition of a drug to a solution of protein

contained in a reaction cell [41]. The formation of ligand-protein complex leads to heat release, which is monitored, and allows to determine the different pharmacokinetics. We keep the candidates with the lowest K_D .

5. In Vivo Validation

After narrowing down potential compounds through *in silico* and *in vitro* screening, the remaining ~6 candidates will undergo *in vivo* validation. This step is crucial for assessing efficacy and evaluating risks and potential off-target effects of our drug in living models. It will additionally allow the determination of optimal doses for upcoming clinical trials in humans, based on pharmacokinetics (PK) and pharmacodynamics (PD).

Only 1 compound and a potential backup compound meeting stringent criteria for efficacy and safety will be selected for clinical trials. Doses and potential off-target effects considered as acceptable will be assessed and tightly monitored for these candidates during clinical trials.

5.1 Animal Selection

Several animal models exist to study AF, including rodents (mice and rats), Göttingen mini pigs, pigs, dogs, sheep and chimpanzees [58].

To select the most pertinent species for each assessment, we first compared PPAR α and PPAR δ expression profiles in potential animal models to those in humans. Using NCBI and Bgee databases (See **Table S6**) as well as studies on PPARs using Göttingen mini pigs, we were able to see that both isoforms of PPARs are expressed in the heart, liver, muscle, brain and kidney of all species [59]–[61]. All of them are thus suitable for our study *in vivo* and translation to humans.

Moreover, the preferred routes of administration of our compounds for *in vivo* studies are oral administration and IV injection as they will be the ones used in humans. They are both available for the mentioned species [62].

Selected animal models for PK and PD investigations include Göttingen minipigs because of their close resemblance to humans in heart size, physiology, and cardiovascular system characteristics as well as their predisposition to arrhythmia [63], [64]. Their ease of handling in a laboratory setting and their less restrictive ethical concerns compared to larger animal models also make them a preferred choice for our study [65]. However, since parts of these assessments as well as toxicity studies require sacrificing several animals, we will also use mice that are more available and cost-effective while still being representative of human physiology [66]. Finally, the efficacy of our compounds will be evaluated both acutely and chronically on German Landrace pigs allowing the use of procedures for larger models such as catheterization and intrathoracic surgery while providing the required information for our study thanks to their cardiac similarities to humans [67], [58]. Despite the absence of spontaneous AF in pigs, they remain suitable for the study thanks to an artificial induction method of rapid atrial heart rates that will be further described called Atrial Tachypacing (ATP) (See Section 5.4) [58].

To be able to perform *in vivo* validation with mice, Göttingen pigs and German Landrace pigs as wanted, Institutional Animal Care and Use Committee (IACUC) approval will be needed. In order to get approval, a detailed research protocol outlining study objectives, methods, and ethical considerations according to local and international regulations will be submitted [68], [69]. Established protocols and guidelines for working with these animal models will be followed to ensure compliance with regulations.

In summary, the workflow will be as indicated in **Figure 5.1**.

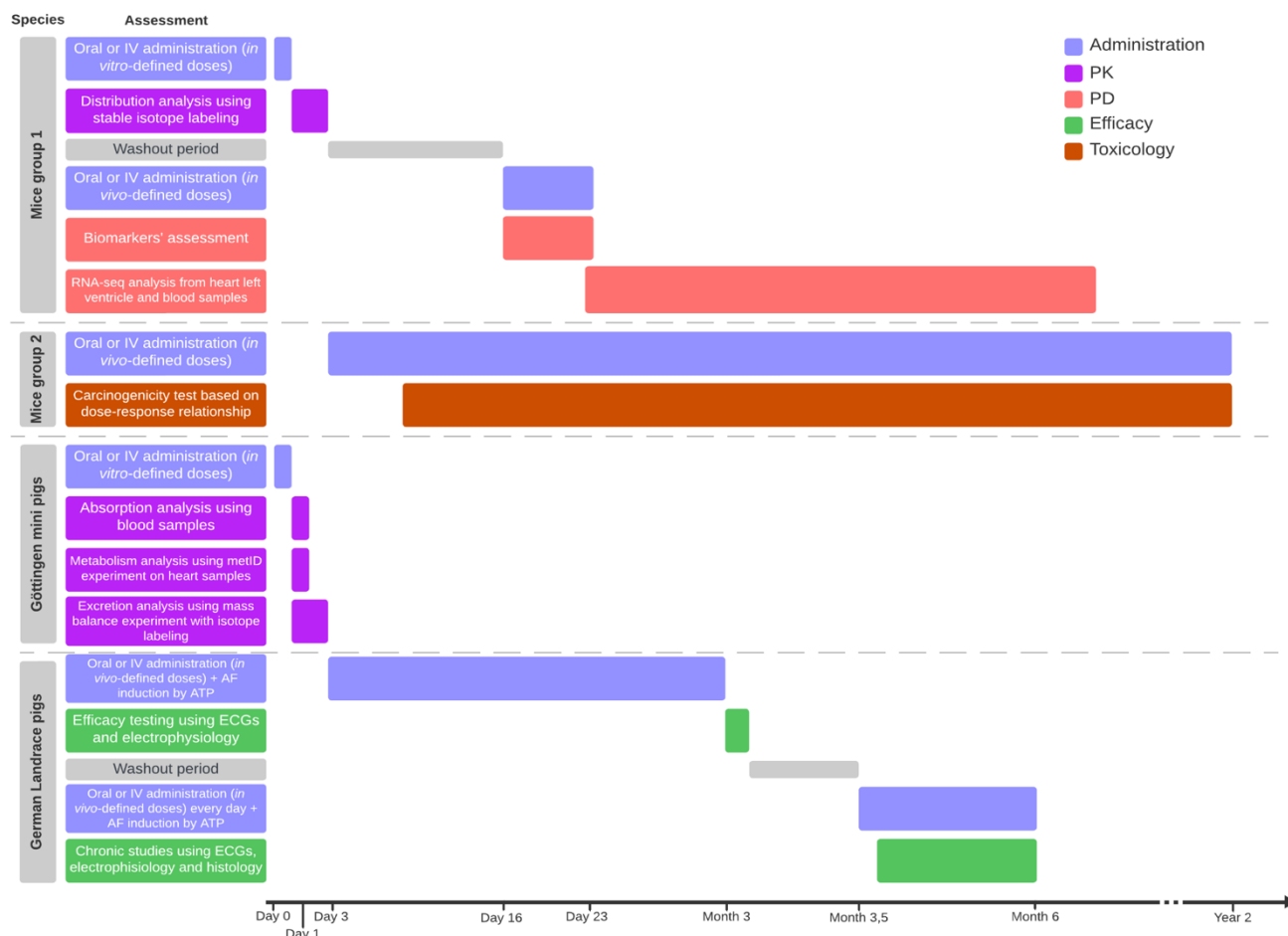


Figure 5.1: In vivo validation workflow. Abbreviations: IV = intravenous; MetID = metabolite identification; AF = atrial fibrillation; ATP = atrial tachypacing; ECG = electrocardiogram; PK = pharmacokinetics; PD = pharmacodynamics

5.2 Pharmacokinetics (PK)

5.2.1 Absorption

Absorption is the process through which the drug is delivered from its administration form to the systemic circulation. Based on a study on Göttingen minipigs on the absorption of paracetamol [70], we will similarly perform an analysis of absorption with both oral dosing and IV administration. We will take the difference in absorption mechanisms between both routes into account. Ultimately, we will reconstruct the curve of the drug plasma concentration by collecting blood samples at several time points after administration ($t = 30 \text{ min}, 1\text{h}, 2\text{h}, 8\text{h}, 24\text{h}$ post-injection) and analyze them by LC-MS/MS. From this plot, we will extract relevant features, such as the area under the curve (AUC), the plasma concentration (C_{\max}), the time to reach C_{\max} (t_{\max}), the half-life ($t_{1/2}$), the clearance (CL) and the bioavailability [63].

5.2.2 Distribution

Distribution reflects how the drug gets spread throughout the body and will be tested by stable isotope labeling [71].

The pre-selected compounds will be tagged with the stable heavy isotope ^{13}C , then orally administered to mice and quantified in different organs of interest at successive time points after administration (every 2h). This will allow us to track the distribution of the drugs across time, as well as to identify the targeted sites. The detection consists in the extraction of cross-sectioned slices from animals, followed by isotopic ratio outlier analysis (IROA) [72]. We will analyze several organs, including the liver, the muscles, the heart and the brain, to assess whether the drug is able to cross the blood-brain barrier (BBB), which is an exclusion criterion, and to assess possible metabolic processing through the hepatic route. From this we will also determine the volume of distribution of the drug (V_d), which will allow us to calculate the loading dose [73].

Supplementary analysis will be performed to assess placental transfer. The principle is simply to administer the isotope labeled drugs to pregnant mice and to subsequently compare the concentration of drug in the maternal and fetal plasma, also at successive time points post-dose [74]. The following steps remain the same. Regardless of the results, pregnancy or intend to conceive will be an exclusion criterion for the initial clinical trial.

5.2.3 Metabolism

Metabolism studies provide insight on how the drug is processed into subsequent compounds. We will carry a metID experiment on heart samples [75], using hydrophilic interaction chromatography (HILIC) for separation, combined with Mass Spectrometry (MS) for identification of the metabolites [76]. This will allow us to determine which metabolites are formed, and to use human-specific toxic metabolites as an exclusion criterion. Based on *in vitro* results, we will select the two drugs expected to interfere the most with our candidate compounds, and assess *in vivo* drug-drug interactions (DDI) by a screening assay [77].

5.2.4 Excretion

Drugs are most commonly excreted from the body through the renal route [73]. Using the same pipeline of ^{13}C isotope labeling [71], we will perform a mass balance experiment [77], [78]. Samples will be collected every 2 hours, up to 48 hours post-administration. We will use ^{13}C labeled glucose as an isotopic internal standard, by administering it through food beforehand [71]. The analysis of the content will be carried via MS analysis. We will consider a passing threshold of 1% of the dose being excreted within a 24-hour period [80].

5.3 Pharmacodynamics (PD)

5.3.1 Biomarkers' Assessment

To further characterize our compound, we will do a preliminary PD study, in conjunction with the preliminary PK study. We will administer each compound both orally and intravenously in 5 healthy mice for 7 days with 5 control mice, to assess the effects of those compounds on the heart and metabolism according to **Table 5.2** [58].

Function to test	Pharmacodynamic parameters	Methods
Heart Rate (HR)	Chronotropic effects	ECG
Blood Pressure (BP)	Changes in blood pressure, both systolic and diastolic	Specialized equipment
Contractility	Force of cardiac muscle contraction	Echocardiography
Simplified Electrocardiogram (ECG or EKG)	Cardiac rhythm, conduction, and repolarization	(ECG or EKG)
Cardiac Output	Amount of blood pumped by the heart per unit of time	Echocardiography or the Fick principle
Vascular Resistance	Resistance to blood flow in the blood vessels	Doppler Ultrasound
Cardioprotective Effects	Protective effects, reducing damage during ischemic events or other	Echocardiography, Histology and Morphometry
Cardiac Hypertrophy	Changes in the size and structure of the heart	Echocardiography, Histological Analysis
Endothelial Function	Function of the endothelium and the inner lining of blood vessels	Wire Myography, Laser Doppler Flowmetry, ...
Inflammatory Markers	Cardiac inflammation	H&E Staining, IHC, ELISA, RT-QPCR
Fibrosis	Fibrotic changes in the heart tissue	Histological examination

Table 5.2: Cardiac functions and toxicity assay on healthy mice [58].

5.3.2 RNA-seq Analysis

Multiple blood biomarkers have been identified in previous studies to diagnose patients susceptible to develop POAF [81]– [84]. We will perform RNAseq on mouse heart left ventricle (LV) and blood samples to determine genes that are up or downregulated upon treatment. Unbiased gene set enrichment analysis will allow us to go from the gene level to the pathway level and thus to determine which pathways are significantly affected upon treatment. RNAseq on LV samples will give us mechanistic insights while RNAseq on blood samples will render the analysis translatable to humans. Thus, blood samples will be retrieved from patients of the clinical trial, before and after treatment, and will be analyzed for differential metabolite

composition. In particular, we will focus on BNP, a marker of myocardial stretch, to analyze the enrichment in that pathway [85].

5.4 Primary Studies for Efficacy

We will use 65 German Landrace pigs (usual amount for *in vivo* testing: 5 for control and 15 for AF testing per compound), aged 3–4 months old and weighing 50–70 kg [86].

As mentioned previously, AF has to be artificially induced by atrial tachypacing (ATP) in pigs. To prevent systolic dysfunction during ATP in swine, AV nodal blockade can be used (e.g., digoxin), which at the end enables the production of over 60 minutes of AF episodes without signs of congestive heart failure (CHF).

Upon the initiation of pacing, pigs were given our drug twice daily with a dosage calculated from the results in section 5.2, orally and intravenously in order to maximize compound diffusion, and digoxin (0.005 to 0.01 mg/kg daily, oral) to slow the ventricular response rate [87]. Prior to pacemaker implantation, swine are initially anesthetized intravenously with usual compounds [87]. A pacemaker is then implanted in the right atria by the internal jugular vein. The pacemaker is programmed to stimulate at 50 Hz for 1s followed by 1s of no stimulation [88]. Every 1 to 2 weeks, the pacemaker is deactivated to determine whether the AF can be sustained for more than 20 minutes, so that it can be used for testing [87], [88].

To test efficacy of the drug we would have to check for different parameters reflecting cardiac functions and assess how well the drugs minimize the effects of induced AF. We plan to look at the variation of stroke volume as the irregular rhythm of AF leads to irregular ventricular filling that should affect the end-systolic volume and, consequently, the cardiac output. It can also modify the heart's afterload, affecting the pressure against which the ventricle must pump. Our compounds should reduce those effects, and the end-systolic elastance should be considerably more comparable to healthy pigs afterwards. End-Systolic Elastance (Ees) study will help us define how ventricular function adapts or deteriorates in response to persistent irregular atrial contractions upon administration of our compounds in addition to providing valuable data about their efficacy. ECG recordings, done via implantation of twelve-lead ECGs and Electrophysiology (EP) measurements will be as shown in **Table 5.3** [86].

Measurements	Normal Range of Values	Atrial fibrillation phenotype
ECG		
P-waves	30 to 70 milliseconds (ms)	Unclearly Defined P-wave
RR interval	600 to 1000 milliseconds (ms)	Irregular and chaotic intervals
PR interval	80 to 120 milliseconds (ms)	Irregularities or the absence of a consistent PR interval
QRS duration	40 to 80 milliseconds (ms)	Unclear ECG
vital signs		
heart rate	60 to 100 beats per minute	Intervals between heartbeats vary unpredictably
QT interval duration	200-400 milliseconds (ms)	Out of the range (not usually used for atrial fibrillation testing)
QTc interval duration	300-500 ms	Out of the range (not usually used for atrial fibrillation testing)
Electrophysiology		
LV volume (ml)	40-75 mL	Global decrease, out of range, or heterogeneous LV volumes
LV pressure (mmHg)	0-100 mmHg	Global decrease, out of range, or heterogeneous LV pressures
End-systolic elastance (Ees)	2 to 5 mmHg.ml ⁻¹	Decrease in end-systolic elastance
Regression line drawn between the end-systolic pressure-volume points of each loop = r²	r ² = 0,99	Decrease overall of r ²

Table 5.3: ECGs and Electrophysiology measurements on pigs.

Catheter-based techniques enable a good proxy of the heart's ability to generate the force needed to eject blood during systole and it can be tested by measuring the contractility of cardiac muscle of the left ventricle (LV). Using a pressure sensor in the catheter, we will register the change in end-systolic pressure-volume relationship (ESPVR) [89]. Here we assess alterations in contractile function by continuously measuring the blood conductivity within the LV. We will

obtain pressure-volume curves during induced AF and an hour after the voltage induction. It is based on those results that we calculate the regression slope of the end-systolic pressure-volume relationship and the end-systolic elastance. For a decreased value of Ees, the LV is able to eject a lower blood volume against the same afterload, which indicates a decreased contractility [90]. Our compounds should then show an unchanged contractility as it reduces occurrence overall.

5.5 Chronic Studies

Chronic POAF represents a burden for patients after surgery. Affected patients show specific activation patterns as overall deterioration in general health: cardiomyopathy, increased risk of heart failure, atrial remodeling, impaired cardiac function [87].

We administer the same dose of drug orally and intravenously every day for 30 days on pigs of the same age and weight as in previous assays. AF episodes are induced as previously by programmed pacemakers, trying to maintain AF for at least 7 days. Once the AF is maintained in the pigs, we check for overall effects with ECGs and electrophysiology measurements as described in **Table 5.3**.

Histology is used to characterize structural changes, as persistent AF leads to structural remodeling of the atria, and fibrosis which could be responsible for the maintenance of arrhythmia. Animals will be euthanized after ~30 days of AF. Tissue samples will be taken from several locations in ventricles, and LV. Samples will then undergo Masson's trichrome staining which enables identifying collagen fibers and other fibrous tissues, characteristic of fibrosis that should not be shown with our compound as it reduces POAF occurrence [87].

5.6 Secondary Studies in Vivo: Toxicology

In some cases, PPAR activation by synthetic compounds might induce tumorigenesis. We will therefore conduct a two-year carcinogenicity study in rodents before proceeding with clinical trials following the timeline in **Table 5.1**, as advised by authorities such as the Food and Drug Administration (FDA) for PPAR agonists [91].

Assessing the results of such a study will involve an assessment of the dose-response relationship, to determine a clear correlation between compound dosing and tumor incidence. We will test for a threshold obtained thanks to data collected in section 5.2, below which no tumors are observed and above which there is an increase in tumor incidence. We will also evaluate the types of observed tumors and the organ specificity.

Finally, the absence of toxicity due to drug interference will have been assured *in vitro* as well as during PK studies.

6. Clinical Trials

6.1 Phase I

Phase I evaluates safety, pharmacokinetics, and the maximum tolerable dose in 21 to 36 (cf. Supplementary Materials) participants equally split between males and females aged 18 to 65. This range excludes the vulnerable elderly while still testing on a broad subgroup of the population. Pregnant women, individuals actively trying to conceive, and those undergoing current treatment are excluded [92]. This phase is anticipated to extend for up to one year.

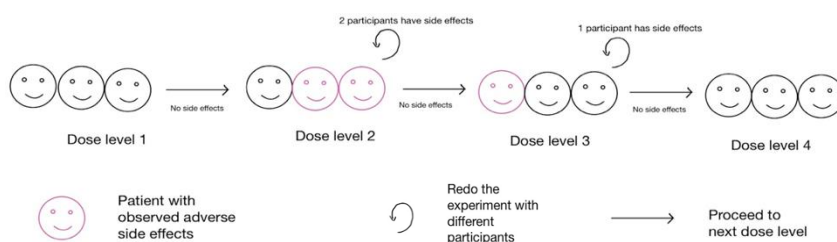


Figure 6.1: Overview of the “3+3” design.

Phase I will use the standard 3+3 design, where each cohort consists of three subjects, across two escalation studies. The first study aims to determine the maximum tolerated dose of the drug [93].

The second study assesses the toxicity upon longer exposure of the drug. Considering that the drug is designed for the acute phase of AF, a single dose, short test will be performed. Four cohorts will be implemented, randomly assigning participants, while keeping them blinded to the dosage level. In line with the 3+3 design (See **Figure 6.1**), cohorts of three patients are assigned to dose levels (See **Tables 6.1** and **6.2**) until one or more dose-limiting toxicities (DLTs) are observed. The DLTs are measured based on pre-defined adverse events during dose escalations [94]. The aim is to determine the maximum tolerated dose and the safety profile of the investigational drug in a small group of participants. If one out of three patients experiences a DLT, three more patients will be assigned to the current dose. The starting dose (SD) will be determined with the body surface area (BSA) normalization method which uses the difference of body surface area between the animal model and humans to adapt the loading dose, determined in section 5.4 [95]. This method has been shown to have a better correlation between various animal models than the conversion based on body weight [95].

Cohort 1	Cohort 2	Cohort 3	Cohort 4
SD	200% of SD	300% of SD	400% of SD

Table 6.1: Dose levels for initial escalation study.

After this first escalation study, a second trial is held to control for the toxicity of the drug upon longer exposure. A 3+3 design is used (**Table 6.2**) [93]. Four cohorts of healthy men and women between 18 and 60 years old receive the treatment for 1 month, followed by 1 month of observation. The timeline for Phase I is presented in **Figure 6.2**.

Cohort 1	Cohort 2	Cohort 3	Cohort 4
25% of MTD	50% of MTD	75% of MTD	100% of MTD

Table 6.2: Dose levels for second escalation study.

Within two weeks after treatment, every patient will be requested to complete a follow-up questionnaire to report any potential side effects related to PPAR agonists administration, such as abdominal discomfort, epigastric pain, nausea, and vomiting.

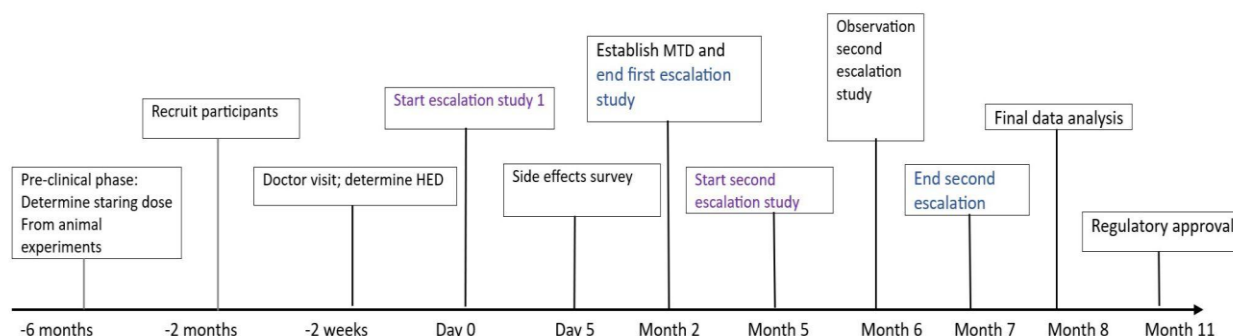


Figure 6.2: Timeline for Phase I of clinical trials.

Test	Reason	Comments
ECG, Blood Pressure, Heart Rate, Echocardiography and Physical Examination [96]	Determine safety and tolerability	ECG is the most deterministic test to diagnose postoperative atrial fibrillation. Done by means of a Holter monitor.
Kansas City Cardiomyopathy Questionnaire (KCCQ)	Determine drug efficacy on daily-life activities and patient well-being	The KCCQ is an FDA-approved assessment of heart failure patients' health through symptoms, physical limitations, social impact and quality of life [97].
6 Minute Walking Test (6MWT), (starting in Phase II)		The 6MWT evaluates exercise tolerance and cardiac response to stress post-surgery [98].
Bicycle Stress Echocardiogram		The Bicycle Stress Echocardiogram measures heart performance at rest and during stress [99].
The Cardiac Rehabilitation Barriers Scale (CRBS)		The CRBS identifies patient barriers to participating in cardiac rehabilitation programs [100].
Blood testing: Albumin, C-reactive protein, creatine kinase, creatinine, calcium, potassium, BNP, troponin, magnesium, phosphate, sodium, urea, uric acid, liver enzymes and bilirubin	Assess safety, tolerability and kidney and liver function	Blood testing can give valuable insights into the functioning of organs and help assess secondary outcome measurements such as acute kidney injury.
Side effects such as abdominal discomfort, epigastric pain, nausea, and vomiting.	Test for common side effects	See in vivo section; PPAR agonists have been associated with cardiotoxicity, hepatotoxicity, gastrointestinal toxicity, and reproductive and developmental toxicity [91]
Cognitive testing: Standardized Mini-Mental Status Exam (SMMSE) and Memory and Executive Screening (MES)	Cognitive function test	AF increases the risk of cognitive impairment and dementia, making cognitive testing vital to understand treatment effects beyond cardiovascular outcomes [101]

Table 6.3: List of the outcome measurements that will be assessed in the clinical trials.

To recruit healthy individuals, we will collaborate with specialized research clinics, healthy volunteer databases, research-ready hospitals, online advertising platforms, patient advocacy groups, and healthcare providers. This multicenter approach aims to boost enrollment, though it may introduce confounding factors into statistical analysis. This decision is, however, necessary due to the limited patient numbers in a single hospital [102].

6.2 Phase II

Phase II aims to assess the efficacy of the drug in patients subjected to potential POAF through the same outcome measures as in Phase I (cf. **Table 6.3**). Additionally, the blood samples will be retrieved and used for RNAseq analysis, as mentioned in section 5.3.2. The primary and secondary outcomes are detailed as follows.

The primary outcome is reducing the incidence of POAF within seven days after surgery [14] by at least 70% compared to the placebo. Preventative β -blockers, which are commonly used for lowering blood pressure and heart rate, have been shown to decrease POAF incidence by 48% [103]. A PPAR δ agonist, initially designed for treatment of acute kidney injury (AKI) post-cardiac surgery, showed a 78% reduction in POAF incidence, suggesting the 70% decrease is realistic [14].

Secondary outcomes include stroke occurrence, AKI, side effects (abdominal discomfort, epigastric pain, nausea, and vomiting), length of hospital stay and death. The diagnosis of AKI can be done through measuring serum creatinine levels (**Table 6.3**) [104], [105].

To assess drug effectiveness, a randomized parallel assignment study is carried out with triple blinding involving a group of 200 men and women (cf. Supplementary Materials). This phase will last up to 2 years. The subjects will be selected based on **Tables 6.4 and 6.5**.

Variable	Criterion	Reason
Age	>40 years old	Most occurrences of AF
Surgery	Having undergone coronary artery bypass graft surgery	Target population for the drug
Informed consent	All patients must be able to provide informed consent to participate in the study	Legally required

Table 6.4: List of the inclusion criteria

Variable	Criterion	Reason
Drug Interactions	Currently taking any drugs except Aspirin, Clopidogrel, β -blockers, Statins or ACE inhibitors [106]	The drug should be compatible with commonly used post-coronary artery bypass graft surgery medications
Previous Diagnosis	Diagnosis prior to surgery of heart arrhythmias (including AFib), stroke, heart failure, COPD, hepatic or renal failure or >2nd degree AV blockade [103],[104]	These patients already have chronic arrhythmias not targeted by the treatment or are at a higher risk of death
Previous Procedures	Splenectomy	Exacerbates atrial inflammatory fibrosis and vulnerability to atrial fibrillation induced by pressure overload [109]
Fertility	Male: Intent to conceive; Female: Pregnant, lactating, not currently on birth control and not menopausal, intent to conceive [110]	The effects on fertility were not evaluated and safety cannot be guaranteed

Table 6.5: List of the exclusion criteria.

Gender	Medical History	Drugs	Qualitative variables
Male, Female	Hypertension, Diabetes, Myocardial infarction, Smoking	Aspirin, Clopidogrel, Statins, ACE inhibitors	Age, BMI, Serum creatinine

Table 6.6: Variables among which the treatment and placebo groups must have roughly the same distributions.

The attributes in **Table 6.6** will be assessed before treatment and statistically evaluated in order to ensure comparable distributions between treatment and placebo group.

Figure 6.3 reports a tentative timeline for outcome measurements. It outlines a preliminary once-daily continuous IV administration for six days post-surgery which is subject to adjustments from pre-clinical trial results.

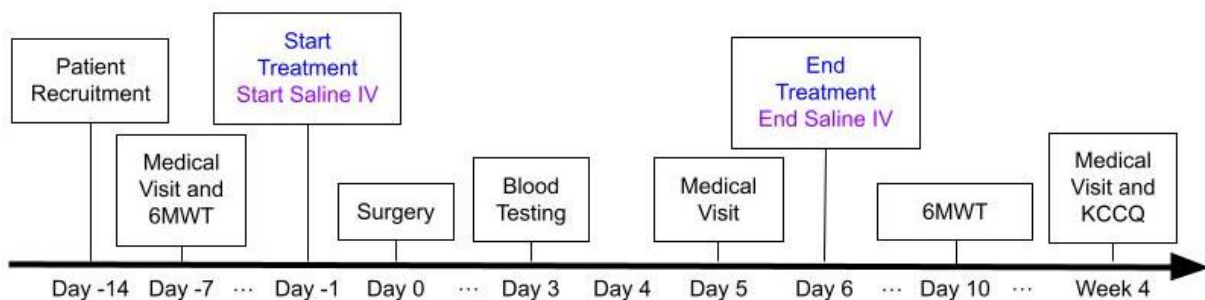


Figure 6.3: Phase II Timeline; Treatment group in blue, control in purple and both in black.

Abbreviations: 6MWT = 6 Minute Walking Test; KCCQ = Kansas City Cardiomyopathy Questionnaire

To assess the effective dosage of the drug, patients will be divided into four randomly assigned subgroups. Each subgroup will be administered a different dosage of the drug in order to obtain the best efficacy while achieving a high level of safety (**Table 6.7**).

Patients will be tested for the same outcomes as evaluated in Phase I. Additionally, they will be asked to report any additional adverse effects. The number of patients discontinuing intervention in both the placebo and treatment group will be assessed during the study.

Cohort 1	Cohort 2	Cohort 3	Cohort 4
25% of Maximum Long-Term Tolerated Dosage	50% of Maximum Long-Term Tolerated Dosage	75% of Maximum Long-Term Tolerated Dosage	100% of Maximum Long-Term Tolerated Dosage

Table 6.7: Best efficacy assessment

6.3 Phase III

Phase III assesses the drug's safety and efficacy over a longer period, screening for rare or long-term side effects. 524 men and women over 40 will be assessed (cf. Supplementary Material). Patients are allocated randomly into two groups receiving a placebo (10% of participants), or the drug. The primary and secondary outcomes are the same as in Phases II and III. After the successful completion of Phase III, the drug can be brought to market.

6.4 Phase IV

Phase IV monitors a drug's long-term safety and efficacy in real-world settings following its market release. It explores safety profiles during extended use and optimal dosing for specific patient groups. This research of at least five years informs label updates and regulatory decisions, with patient feedback contributing to assessments of tolerability and effectiveness in real-life situations and scrutinizes the drug's economic impact. Phase IV is vital for ensuring safety, guiding healthcare practices, and enhancing public health.

7. Business Plan

Executive Summary: Rythmiar targets postoperative atrial fibrillation (POAF) and has potential applications in acute kidney injury (AKI) and chronic atrial fibrillation. Proven effective and safe in clinical trials, it initially targets patients over 40 undergoing coronary artery bypass graft surgery.

Market Analysis: POAF occurs in 20-40% of cardiac surgical procedures [2] representing a significant market opportunity. Apart from heightened risk of stroke, thromboembolism, and mortality, POAF also increases the duration of hospital stay, imposing a serious burden on the healthcare system as well as the patient [111].

The drug will first gain market approval through the FDA in the US before the market is expanded worldwide to increase revenue further. The future expansion to other surgeries, AKI and Chronic Atrial Fibrillation enhances the drug's potential market further. Our drug targets an unmet need for specialized treatments in these areas.

Product Description: Rythmiar works by targeting fatty acid metabolism in the heart through PPAR α and PPAR δ interaction, offering a new approach to manage POAF. It will be administered via continuous infusion pre- and post-operatively, with an oral formulation in development (See **Table 2.1**). The drug reduces atrial fibrillation (AF) incidence by at least 70% and, therefore, also minimizes associated complications like stroke and prolonged hospital stays.

Financial: POAF affects 20-40% of the 400k cardiac surgical procedures conducted annually in the United States [112]. The condition presents not only a substantial health concern but also a notable economic burden. Managing POAF costs an average of \$15k [113], translating to an estimated Total Addressable Market (TAM) of approximately \$1.8B each year. With a conservative estimate of achieving a 20% market penetration, the Serviceable Available Market (SAM) for Rythmiar is projected to be around \$360M annually.

In terms of pricing strategy, Rythmiar is set at \$7k for the complete treatment, or \$875 per dose. This pricing considers the drug's high efficacy rate. The cost efficiency of Rythmiar is further

bolstered by its production costs. Estimated at \$2 per dose [114], [115] and factoring in an additional 25% for contract manufacturing, the total production cost amounts to \$2.50 per dose allowing for a substantial profit margin of \$872.50 per dose.

In order to become profitable, the drug will need to break even on the development costs. The pre-clinical studies have an estimated cost of \$1.2M [116]. The most substantial expense in developing Rythmiar will be the clinical trials. With the average cost of \$39,857 per patient in cardiovascular trials [117], our planned clinical phases 1 to 3 will lead to an estimated total cost of approximately \$37.5M. Taking the total development cost as \$38.7M a break-even point of about 45k doses or 5.5k treatment courses can be calculated. Given the estimated market penetration rate this should be achieved in a little over a month post market release. With the expansion to other applications of the drug the market size and revenue are expected to grow further.

8. Conclusion

Atrial fibrillation is associated with mitochondrial dysfunction. Specifically, this involves a disruption in fatty acid oxidation (FAO), which impairs energy production, as this process is the primary source of ATP. Efficient FAO ensures a steady energy supply, minimizing cardiac stress and thereby reducing the risk of arrhythmias, particularly atrial fibrillation. Targeting peroxisome proliferator-activated receptors (PPARs), namely PPAR α and PPAR δ , emerges as a promising strategy to alleviate postoperative atrial fibrillation (POAF) and address heart-specific concerns. We employed *in silico* methods to discover a PPAR α/δ dual agonist, facilitating efficient screening and optimization of potential drug candidates before experimental testing. Subsequently, we validated the compound's efficiency through *in vitro* studies, consisting in primary assays to assess solubility, lipophilicity, permeability, and toxicity, along with secondary assays targeting genotoxicity and cardiotoxicity. We proceeded to conduct *in vivo* studies to further evaluate the compound's efficacy and safety in a living organism, such as mice, Göttingen pigs and German Landrace pigs. Finally, we advanced through four phases of clinical trials, administering the drug intravenously to patients undergoing coronary artery graft bypass surgery through an 8-day once-daily infusion during their in-hospital stay for the acute phase of atrial fibrillation. Upon release, the drug is expected to have a break-even point of about 48 '000 doses.

Furthermore, we intend to expand the scope of this drug for chronic atrial fibrillation (AF), necessitating a transition to daily oral administration. Additionally, the established effectiveness of PPAR δ agonists in treating Acute Kidney Injury (AKI) post-cardiac surgery suggests potential benefits for our product in addressing this disease. Given the emerging research on the connection between mitochondrial dysfunctionality and heart diseases, coupled with our drug's efficacy, there is exploration potential for its application in other forms of heart diseases and various surgeries, including valvular surgery and non-cardiac surgeries [118]. However, these extensions, including chronic atrial fibrillation, AKI, other types of surgery, and various heart diseases, will require further assessments.

9. Bibliography

- [1] J. Jeganathan et al., "Mitochondrial Dysfunction in Atrial Tissue of Patients Developing Postoperative Atrial Fibrillation," *Ann. Thorac. Surg.*, vol. 104, no. 5, pp. 1547–1555, Nov. 2017, doi: 10.1016/j.athoracsur.2017.04.060.
- [2] D. Dobrev, M. Aguilar, J. Heijman, J.-B. Guichard, and S. Nattel, "Postoperative atrial fibrillation: mechanisms, manifestations and management," *Nat. Rev. Cardiol.*, vol. 16, no. 7, pp. 417–436, Jul. 2019, doi: 10.1038/s41569-019-0166-5.
- [3] C. J. M. van Opbergen, L. den Braven, M. Delmar, and T. A. B. van Veen, "Mitochondrial Dysfunction as Substrate for Arrhythmogenic Cardiomyopathy: A Search for New Disease Mechanisms," *Front. Physiol.*, vol. 10, 2019, Accessed: Nov. 19, 2023. [Online]. Available: <https://www.frontiersin.org/articles/10.3389/fphys.2019.01496>
- [4] M. K. Turagam, F. X. Downey, D. C. Kress, J. Sra, A. J. Tajik, and A. Jahangir, "Pharmacological strategies for prevention of postoperative atrial fibrillation," *Expert Rev. Clin. Pharmacol.*, vol. 8, no. 2, pp. 233–250, Mar. 2015, doi: 10.1586/17512433.2015.1018182.
- [5] I. F. Kodde, J. van der Stok, R. T. Smolenski, and J. W. de Jong, "Metabolic and genetic regulation of cardiac energy substrate preference," *Comp. Biochem. Physiol. A. Mol. Integr. Physiol.*, vol. 146, no. 1, pp. 26–39, Jan. 2007, doi: 10.1016/j.cbpa.2006.09.014.
- [6] V. Saks, R. Favier, R. Guzun, U. Schlattner, and T. Wallimann, "Molecular system bioenergetics: regulation of substrate supply in response to heart energy demands," *J. Physiol.*, vol. 577, no. Pt 3, pp. 769–777, Dec. 2006, doi: 10.1113/jphysiol.2006.120584.
- [7] L. Pool, L. F. J. M. Wijdeveld, N. M. S. de Groot, and B. J. J. M. Brundel, "The Role of Mitochondrial Dysfunction in Atrial Fibrillation: Translation to Druggable Target and Biomarker Discovery," *Int. J. Mol. Sci.*, vol. 22, no. 16, p. 8463, Aug. 2021, doi: 10.3390/ijms22168463.
- [8] A. Grynberg and L. Demaison, "Fatty acid oxidation in the heart," *J. Cardiovasc. Pharmacol.*, vol. 28 Suppl 1, pp. S11-17, 1996, doi: 10.1097/00005344-199600003-00003.
- [9] D. Namgaladze and B. Brüne, "Macrophage fatty acid oxidation and its roles in macrophage polarization and fatty acid-induced inflammation," *Biochim. Biophys. Acta*, vol. 1861, no. 11, pp. 1796–1807, Nov. 2016, doi: 10.1016/j.bbalip.2016.09.002.
- [10] M. Hamblin, L. Chang, Y. Fan, J. Zhang, and Y. E. Chen, "PPARs and the Cardiovascular System," *Antioxid. Redox Signal.*, vol. 11, no. 6, pp. 1415–1452, Jun. 2009, doi: 10.1089/ars.2008.2280.
- [11] B. Grygiel-Górniak, "Peroxisome proliferator-activated receptors and their ligands: nutritional and clinical implications - a review," *Nutr. J.*, vol. 13, no. 1, p. 17, Feb. 2014, doi: 10.1186/1475-2891-13-17.
- [12] J. G. Duncan and B. N. Finck, "The PPAR<svg style='vertical-align:-0.216pt;width:12.8625px;' id='M1' height='10.4375' version='1.1' viewBox='0 0 12.8625 10.4375' width='12.8625' xmlns:xlink='http://www.w3.org/1999/xlink' xmlns='http://www.w3.org/2000/svg'> <g transform='matrix(.022,-0,0,-.022,.062,10.1)'><path id='x1D6FC' d='M545 106q-67 -118 -134 -118q-24 0 -40 37.5t-30 129.5h-2q-47 -72 -103 -119.5t-108 -47.5q-47 0 -76 45.5t-29 119.5q0 113 85 204t174 91q47 0 70 -33.5t43 -119.5h3q32 47 80 140l55 13l10 -9q-47 -80 -138 -201q17 -99 27.5 -136t22.5 -37q23 0 69 61zM333 204 q-14 98 -31 149.5t-50 51.5q-49 0 -94 -70t-45 -164q0 -55 15.5 -86t40.5 -31q70 0 164 150z' /></g> </svg>-PGC-1<svg style='vertical-align:-0.216pt;width:12.8625px;' id='M2' height='10.4375' version='1.1' viewBox='0 0 12.8625 10.4375' width='12.8625' xmlns:xlink='http://www.w3.org/1999/xlink' xmlns='http://www.w3.org/2000/svg'> <g transform='matrix(.022,-0,0,-.022,.062,10.1)'><use xlink:href='#x1D6FC' /></g> </svg> Axis Controls Cardiac Energy Metabolism in Healthy and Diseased Myocardium," *PPAR Res.*, vol. 2008, p. e253817, Nov. 2007, doi: 10.1155/2008/253817.
- [13] T. E. Miller and P. S. Myles, "Perioperative Fluid Therapy for Major Surgery," *Anesthesiology*, vol. 130, no. 5, pp. 825–832, May 2019, doi: 10.1097/ALN.0000000000002603.
- [14] J. W. O. van Till et al., "The Effects of Peroxisome Proliferator-Activated Receptor-Delta Modulator ASP1128 in Patients at Risk for Acute Kidney Injury Following Cardiac Surgery," *Kidney Int. Rep.*, vol. 8, no. 7, pp. 1407–1416, Jul. 2023, doi: 10.1016/j.ekir.2023.04.004.

- [15] H.-X. Chen et al., "Role of the PPAR pathway in atrial fibrillation associated with heart valve disease: transcriptomics and proteomics in human atrial tissue," *Signal Transduct. Target. Ther.*, vol. 5, no. 1, Art. no. 1, Jan. 2020, doi: 10.1038/s41392-019-0093-2.
- [16] D. Giordano, C. Biancaniello, M. A. Argenio, and A. Facchiano, "Drug Design by Pharmacophore and Virtual Screening Approach," *Pharmaceuticals*, vol. 15, no. 5, Art. no. 5, May 2022, doi: 10.3390/ph15050646.
- [17] T. A. de Oliveira, M. P. da Silva, E. H. B. Maia, A. M. da Silva, and A. G. Taranto, "Virtual Screening Algorithms in Drug Discovery: A Review Focused on Machine and Deep Learning Methods," *Drugs Drug Candidates*, vol. 2, no. 2, Art. no. 2, Jun. 2023, doi: 10.3390/ddc2020017.
- [18] "UniProt Knowledgebase (UniProtKB) | UniProt." Accessed: Nov. 27, 2023. [Online]. Available: <https://www.uniprot.org/uniprotkb>
- [19] R. P. D. Bank, "RCSB PDB: Homepage." Accessed: Nov. 27, 2023. [Online]. Available: <https://www.rcsb.org/>
- [20] R. P. D. Bank, "RCSB PDB - 1K7L: The 2.5 Angstrom resolution crystal structure of the human PPAR α ligand binding domain bound with GW409544 and a co-activator peptide." Accessed: Nov. 27, 2023. [Online]. Available: <https://www.rcsb.org/structure/1k7l>
- [21] R. P. D. Bank, "RCSB PDB - 3TKM: Crystal structure PPAR delta binding GW0742." Accessed: Nov. 27, 2023. [Online]. Available: <https://www.rcsb.org/structure/3TKM>
- [22] J. Jumper et al., "Highly accurate protein structure prediction with AlphaFold," *Nature*, vol. 596, no. 7873, Art. no. 7873, Aug. 2021, doi: 10.1038/s41586-021-03819-2.
- [23] M. Varadi et al., "AlphaFold Protein Structure Database: massively expanding the structural coverage of protein-sequence space with high-accuracy models," *Nucleic Acids Res.*, vol. 50, no. D1, pp. D439–D444, Jan. 2022, doi: 10.1093/nar/gkab1061.
- [24] J. Yang, A. Roy, and Y. Zhang, "Protein-ligand binding site recognition using complementary binding-specific substructure comparison and sequence profile alignment," *Bioinforma. Oxf. Engl.*, vol. 29, no. 20, pp. 2588–2595, Oct. 2013, doi: 10.1093/bioinformatics/btt447.
- [25] J. Yang, A. Roy, and Y. Zhang, "BioLiP: a semi-manually curated database for biologically relevant ligand-protein interactions," *Nucleic Acids Res.*, vol. 41, no. Database issue, pp. D1096–1103, Jan. 2013, doi: 10.1093/nar/gks966.
- [26] S. Kamata et al., "PPAR α Ligand-Binding Domain Structures with Endogenous Fatty Acids and Fibrates," *iScience*, vol. 23, no. 11, p. 101727, Oct. 2020, doi: 10.1016/j.isci.2020.101727.
- [27] J. Shang et al., "A molecular switch regulating transcriptional repression and activation of PPAR γ ," *Nat. Commun.*, vol. 11, no. 1, Art. no. 1, Feb. 2020, doi: 10.1038/s41467-020-14750-x.
- [28] "PyMOL | pymol.org." Accessed: Nov. 27, 2023. [Online]. Available: <https://pymol.org/2/>
- [29] P. García, P. Lorenzo, and A. R. de Lera, "Chapter Nine - Natural ligands of RXR receptors," in *Methods in Enzymology*, vol. 637, E. Pohl, Ed., in *Retinoid Signaling Pathways*, vol. 637, Academic Press, 2020, pp. 209–234. doi: 10.1016/bs.mie.2020.02.006.
- [30] D. Douguet, E. Thoreau, and G. Grassy, "<https://chemoinfo.ipmc.cnrs.fr/LEA3D/index.html>," *J. Comput. Aided Mol. Des.*, vol. 14, no. 5, pp. 449–466, 2000, doi: 10.1023/A:1008108423895.
- [31] D. Douguet, "e-LEA3D: a computational-aided drug design web server," *Nucleic Acids Res.*, vol. 38, no. Web Server issue, pp. W615–621, Jul. 2010, doi: 10.1093/nar/gkq322.
- [32] D. Douguet, H. Munier-Lehmann, G. Labesse, and S. Pochet, "LEA3D: A Computer-Aided Ligand Design for Structure-Based Drug Design," *J. Med. Chem.*, vol. 48, no. 7, pp. 2457–2468, Apr. 2005, doi: 10.1021/jm0492296.
- [33] L. Z. Benet, C. M. Hosey, O. Ursu, and T. I. Oprea, "BDDCS, the Rule of 5 and drugability," *Adv. Drug Deliv. Rev.*, vol. 101, pp. 89–98, Jun. 2016, doi: 10.1016/j.addr.2016.05.007.
- [34] O. Korb, T. Stützel, and T. E. Exner, "Empirical Scoring Functions for Advanced Protein–Ligand Docking with PLANTS," *J. Chem. Inf. Model.*, vol. 49, no. 1, pp. 84–96, Jan. 2009, doi: 10.1021/ci800298z.
- [35] S. L. Dixon, A. M. Smondyrev, E. H. Knoll, S. N. Rao, D. E. Shaw, and R. A. Friesner, "PHASE: a new engine for pharmacophore perception, 3D QSAR model development, and 3D database screening: 1. Methodology and preliminary results," *J. Comput. Aided Mol. Des.*, vol. 20, no. 10–11, pp. 647–671, 2006, doi: 10.1007/s10822-006-9087-6.

- [36] S. L. Dixon, A. M. Smondyrev, and S. N. Rao, "PHASE: a novel approach to pharmacophore modeling and 3D database searching," *Chem. Biol. Drug Des.*, vol. 67, no. 5, pp. 370–372, May 2006, doi: 10.1111/j.1747-0285.2006.00384.x.
- [37] V. Venkatraman et al., "Drugsniffer: An Open Source Workflow for Virtually Screening Billions of Molecules for Binding Affinity to Protein Targets," *Front. Pharmacol.*, vol. 13, p. 874746, 2022, doi: 10.3389/fphar.2022.874746.
- [38] H. van de Waterbeemd and E. Gifford, "ADMET in silico modelling: towards prediction paradise?," *Nat. Rev. Drug Discov.*, vol. 2, no. 3, Art. no. 3, Mar. 2003, doi: 10.1038/nrd1032.
- [39] V. Venkatraman, "FP-ADMET: a compendium of fingerprint-based ADMET prediction models," *J. Cheminformatics*, vol. 13, no. 1, p. 75, Dec. 2021, doi: 10.1186/s13321-021-00557-5.
- [40] S. Jo, T. Kim, V. G. Iyer, and W. Im, "CHARMM-GUI: a web-based graphical user interface for CHARMM," *J. Comput. Chem.*, vol. 29, no. 11, pp. 1859–1865, Aug. 2008, doi: 10.1002/jcc.20945.
- [41] K. Vuignier, J. Schappler, J.-L. Veuthey, P.-A. Carrupt, and S. Martel, "Drug-protein binding: a critical review of analytical tools," *Anal. Bioanal. Chem.*, vol. 398, no. 1, pp. 53–66, Sep. 2010, doi: 10.1007/s00216-010-3737-1.
- [42] D. S. Hage, "High-performance affinity chromatography: a powerful tool for studying serum protein binding," *J. Chromatogr. B Analyt. Technol. Biomed. Life. Sci.*, vol. 768, no. 1, pp. 3–30, Feb. 2002, doi: 10.1016/s0378-4347(01)00482-0.
- [43] S. V. Rao, K. W. Anderson, and L. G. Bachas, "Oriented immobilization of proteins," *Microchim. Acta*, vol. 128, no. 3, pp. 127–143, Sep. 1998, doi: 10.1007/BF01243043.
- [44] L. A. A. de Jong, D. R. A. Uges, J. P. Franke, and R. Bischoff, "Receptor–ligand binding assays: Technologies and Applications," *J. Chromatogr. B*, vol. 829, no. 1, pp. 1–25, Dec. 2005, doi: 10.1016/j.jchromb.2005.10.002.
- [45] J. Ponmozhi et al., "Development of Skin-On-A-Chip Platforms for Different Utilizations: Factors to Be Considered," *Micromachines*, vol. 12, no. 3, p. 294, Mar. 2021, doi: 10.3390/mi12030294.
- [46] T. Riss, A. Niles, R. Moravec, N. Karassina, and J. Vidugiriene, "Cytotoxicity Assays: In Vitro Methods to Measure Dead Cells," in *Assay Guidance Manual*, S. Markossian, A. Grossman, K. Brimacombe, M. Arkin, D. Auld, C. Austin, J. Baell, T. D. Y. Chung, N. P. Coussens, J. L. Dahlin, V. Devanarayan, T. L. Foley, M. Glicksman, K. Gorshkov, J. V. Haas, M. D. Hall, S. Hoare, J. Inglese, P. W. Iversen, S. C. Kales, M. Lal-Nag, Z. Li, J. McGee, O. McManus, T. Riss, P. Saradjian, G. S. Sittampalam, M. Tarselli, O. J. Trask, Y. Wang, J. R. Weidner, M. J. Wildey, K. Wilson, M. Xia, and X. Xu, Eds., Bethesda (MD): Eli Lilly & Company and the National Center for Advancing Translational Sciences, 2004. Accessed: Nov. 19, 2023. [Online]. Available: <http://www.ncbi.nlm.nih.gov/books/NBK540958/>
- [47] "Micronucleus Test - an overview | ScienceDirect Topics." Accessed: Nov. 27, 2023. [Online]. Available: <https://www.sciencedirect.com/topics/immunology-and-microbiology/micronucleus-test>
- [48] "AC16 Human Cardiomyocyte Cell Line Millipore." Accessed: Nov. 20, 2023. [Online]. Available: <http://www.sigmaaldrich.com/>
- [49] "HepaRG | Lonza." Accessed: Nov. 20, 2023. [Online]. Available: https://bioscience.lonza.com/lonza_bs/CH/en/Primary-and-Stem-Cells/p/000000000000222176/NoSpin-HepaRG-%288-0M-cells-vial%29
- [50] S. Tejs, "The Ames test: a methodological short review," *Env. Biotechnol*, vol. 4, Jan. 2008.
- [51] "Ames test," Wikipedia. Nov. 08, 2023. Accessed: Nov. 19, 2023. [Online]. Available: https://en.wikipedia.org/w/index.php?title=Ames_test&oldid=1184068878
- [52] "In Vitro Methods in Pharmaceutical Research - 1st Edition." Accessed: Nov. 19, 2023. [Online]. Available: <https://shop.elsevier.com/books/in-vitro-methods-in-pharmaceutical-research/castell/978-0-12-163390-5>
- [53] C. R. C. Wyndham, "Atrial Fibrillation: The Most Common Arrhythmia," *Tex. Heart Inst. J.*, vol. 27, no. 3, pp. 257–267, 2000.
- [54] "Shake-Flask Solubility Assay | Bienta." Accessed: Nov. 19, 2023. [Online]. Available: <https://bienta.net/shake-flask-solubility/>

- [55] A. Andrés et al., "Setup and validation of shake-flask procedures for the determination of partition coefficients (logD) from low drug amounts," *Eur. J. Pharm. Sci. Off. J. Eur. Fed. Pharm. Sci.*, vol. 76, pp. 181–191, Aug. 2015, doi: 10.1016/j.ejps.2015.05.008.
- [56] "Permeability and Absorption - Creative Biolabs." Accessed: Nov. 19, 2023. [Online]. Available: <https://www.creative-biolabs.com/drug-discovery/therapeutics/permeability-and-absorption.htm>
- [57] X. Hakim, "Structure of Synthetic Membrane and Its Classification".
- [58] D. Schüttler et al., "Animal Models of Atrial Fibrillation," *Circ. Res.*, vol. 127, no. 1, pp. 91–110, Jun. 2020, doi: 10.1161/CIRCRESAHA.120.316366.
- [59] "PPAR - Gene - NCBI." Accessed: Nov. 19, 2023. [Online]. Available: <https://www.ncbi.nlm.nih.gov/gene/?term=PPAR>
- [60] "PPAR - Gene search." Accessed: Nov. 30, 2023. [Online]. Available: <https://www.bgee.org/search/genes?search=PPAR>
- [61] P. Yongming et al., "Involvement of peroxisome proliferator-activated receptors in cardiac and vascular remodeling in a novel minipig model of insulin resistance and atherosclerosis induced by consumption of a high-fat/cholesterol diet," *Cardiovasc. Diabetol.*, vol. 14, p. 6, Jan. 2015, doi: 10.1186/s12933-014-0165-0.
- [62] P. V. Turner, T. Brabb, C. Pekow, and M. A. Vasbinder, "Administration of Substances to Laboratory Animals: Routes of Administration and Factors to Consider," *J. Am. Assoc. Lab. Anim. Sci. JAALAS*, vol. 50, no. 5, pp. 600–613, Sep. 2011.
- [63] H. Yoshimatsu, Y. Konno, K. Ishii, M. Satsukawa, and S. Yamashita, "Usefulness of minipigs for predicting human pharmacokinetics: Prediction of distribution volume and plasma clearance," *Drug Metab. Pharmacokinet.*, vol. 31, no. 1, pp. 73–81, Feb. 2016, doi: 10.1016/j.dmpk.2015.11.001.
- [64] A. Stricker-Krongrad, C. Shoemaker, D. Brocksmith, J. Liu, R. Hamlin, and G. Bouchard, "Comparative cardiovascular physiology and pathology in selected lineages of minipigs: Relation to drug safety evaluation," *Toxicol. Res. Appl.*, vol. 1, p. 239784731769636, Mar. 2017, doi: 10.1177/2397847317696367.
- [65] G. Jeppesen and M. Skydsgaard, "Spontaneous background pathology in Göttingen minipigs," *Toxicol. Pathol.*, vol. 43, no. 2, pp. 257–266, Feb. 2015, doi: 10.1177/0192623314538344.
- [66] E. C. Bryda, "The Mighty Mouse: The Impact of Rodents on Advances in Biomedical Research," *Mo. Med.*, vol. 110, no. 3, pp. 207–211, 2013.
- [67] D. Schüttler et al., "A practical guide to setting up pig models for cardiovascular catheterization, electrophysiological assessment and heart disease research," *Lab Anim.*, vol. 51, no. 2, Art. no. 2, Feb. 2022, doi: 10.1038/s41684-021-00909-6.
- [68] M. National Research Council (US) Committee to Update Science, "Regulation of Animal Research," in *Science, Medicine, and Animals*, National Academies Press (US), 2004. Accessed: Nov. 19, 2023. [Online]. Available: <https://www.ncbi.nlm.nih.gov/books/NBK24650/>
- [69] "Institutional Animal Care and Use Committee - an overview | ScienceDirect Topics." Accessed: Nov. 19, 2023. [Online]. Available: <https://www.sciencedirect.com/topics/agricultural-and-biological-sciences/institutional-animal-care-and-use-committee>
- [70] C. Suenderhauf, G. Tuffin, H. Lorentsen, H.-P. Grimm, C. Flament, and N. Parrott, "Pharmacokinetics of Paracetamol in Göttingen Minipigs: In Vivo Studies and Modeling to Elucidate Physiological Determinants of Absorption," *Pharm. Res.*, vol. 31, no. 10, pp. 2696–2707, Oct. 2014, doi: 10.1007/s11095-014-1367-6.
- [71] C. Jang, L. Chen, and J. D. Rabinowitz, "Metabolomics and Isotope Tracing," *Cell*, vol. 173, no. 4, pp. 822–837, May 2018, doi: 10.1016/j.cell.2018.03.055.
- [72] "Phosphor Imaging," Azure Biosystems. Accessed: Nov. 19, 2023. [Online]. Available: <https://azurebiosystems.com/western-blotting-applications/phosphor-imaging/>
- [73] S. Grogan and C. V. Preuss, "Pharmacokinetics," in *StatPearls, Treasure Island (FL): StatPearls Publishing*, 2023. Accessed: Nov. 19, 2023. [Online]. Available: <http://www.ncbi.nlm.nih.gov/books/NBK557744/>
- [74] G. M. Pacifici and R. Nottoli, "Placental Transfer of Drugs Administered to the Mother," *Clin. Pharmacokinet.*, vol. 28, no. 3, pp. 235–269, Mar. 1995, doi: 10.2165/00003088-199528030-00005.

- [75] "MetID: In Vivo Metabolite Identification," XenoTech. Accessed: Nov. 19, 2023. [Online]. Available: <https://www.xenotech.com/preclinical-drug-development/in-vivo-adme-pk-studies/met-id/>
- [76] T. Züllig, M. Zandl-Lang, M. Trötz Müller, J. Hartler, B. Plecko, and H. C. Köfeler, "A Metabolomics Workflow for Analyzing Complex Biological Samples Using a Combined Method of Untargeted and Target-List Based Approaches," *Metabolites*, vol. 10, no. 9, p. 342, Aug. 2020, doi: 10.3390/metabo10090342.
- [77] C. Lu and L. Di, "In vitro and in vivo methods to assess pharmacokinetic drug– drug interactions in drug discovery and development," *Biopharm. Drug Dispos.*, vol. 41, no. 1–2, pp. 3–31, 2020, doi: 10.1002/bdd.2212.
- [78] "Excretion Studies for In Vivo ADME in Drug Development," XenoTech. Accessed: Nov. 19, 2023. [Online]. Available: <https://www.xenotech.com/preclinical-drug-development/in-vivo-adme-pk-studies/excretion/>
- [79] "Liquid Scintillation Counting | LSC Analysis," PerkinElmer. Accessed: Nov. 19, 2023. [Online]. Available: <https://www.perkinelmer.com/lab-products-and-services/application-support-knowledgebase/radiometric/liquid-scintillation-counting.html>
- [80] E. M. Isin, C. S. Elmore, G. N. Nilsson, R. A. Thompson, and L. Weidolf, "Use of Radiolabeled Compounds in Drug Metabolism and Pharmacokinetic Studies," *Chem. Res. Toxicol.*, vol. 25, no. 3, pp. 532–542, Mar. 2012, doi: 10.1021/tx2005212.
- [81] M. S. Khan, K. Yamashita, V. Sharma, R. Ranjan, C. H. Selzman, and D. J. Dossdall, "Perioperative Biomarkers Predicting Postoperative Atrial Fibrillation Risk After Coronary Artery Bypass Grafting: A Narrative Review," *J. Cardiothorac. Vasc. Anesth.*, vol. 34, no. 7, pp. 1933–1941, Jul. 2020, doi: 10.1053/j.jvca.2019.09.022.
- [82] K.-W. Chang, J. C. Hsu, A. Toomu, S. Fox, and A. S. Maisel, "Clinical Applications of Biomarkers in Atrial Fibrillation," *Am. J. Med.*, vol. 130, no. 12, pp. 1351–1357, Dec. 2017, doi: 10.1016/j.amjmed.2017.08.003.
- [83] D. Kaireviciute et al., "Characterisation and validity of inflammatory biomarkers in the prediction of post-operative atrial fibrillation in coronary artery disease patients," *Thromb. Haemost.*, vol. 104, no. 7, pp. 122–127, 2010, doi: 10.1160/TH09-12-0837.
- [84] M. K. Turagam et al., "Circulating Biomarkers Predictive of Postoperative Atrial Fibrillation," *Cardiol. Rev.*, vol. 24, no. 2, pp. 76–87, 2016, doi: 10.1097/CRD.0000000000000059.
- [85] A. H. Bruggink et al., "Brain natriuretic peptide is produced both by cardiomyocytes and cells infiltrating the heart in patients with severe heart failure supported by a left ventricular assist device," *J. Heart Lung Transplant. Off. Publ. Int. Soc. Heart Transplant.*, vol. 25, no. 2, pp. 174–180, Feb. 2006, doi: 10.1016/j.healun.2005.09.007.
- [86] S. Clauss et al., "Characterization of a porcine model of atrial arrhythmogenicity in the context of ischaemic heart failure," *PLoS ONE*, vol. 15, no. 5, p. e0232374, May 2020, doi: 10.1371/journal.pone.0232374.
- [87] D. J. Dossdall et al., "Chronic atrial fibrillation causes left ventricular dysfunction in dogs but not goats: experience with dogs, goats, and pigs," *Am. J. Physiol.-Heart Circ. Physiol.*, vol. 305, no. 5, pp. H725–H731, Sep. 2013, doi: 10.1152/ajpheart.00440.2013.
- [88] K. A. S. Silva and C. A. Emter, "Large Animal Models of Heart Failure: A Translational Bridge to Clinical Success," *JACC Basic Transl. Sci.*, vol. 5, no. 8, pp. 840–856, Aug. 2020, doi: 10.1016/j.jacbts.2020.04.011.
- [89] M. E. Lewis et al., "Vagus nerve stimulation decreases left ventricular contractility in vivo in the human and pig heart," *J. Physiol.*, vol. 534, no. Pt 2, pp. 547–552, Jul. 2001, doi: 10.1111/j.1469-7793.2001.00547.x.
- [90] V. Bikia et al., "Estimation of Left Ventricular End-Systolic Elastance From Brachial Pressure Waveform via Deep Learning," *Front. Bioeng. Biotechnol.*, vol. 9, p. 754003, Oct. 2021, doi: 10.3389/fbioe.2021.754003.
- [91] Y. Xi, Y. Zhang, S. Zhu, Y. Luo, P. Xu, and Z. Huang, "PPAR-Mediated Toxicology and Applied Pharmacology," *Cells*, vol. 9, no. 2, p. 352, Feb. 2020, doi: 10.3390/cells9020352.
- [92] UCSF, "UCSF Atrial Fibrillation Trial: Single Arm Open Label Study of the FARAPULSE Pulsed Field Ablation System in Subjects With Persistent Atrial Fibrillation." Accessed: Nov. 19, 2023. [Online]. Available: <https://clinicaltrials.ucsf.edu/trial/NCT05443594>

- [93] G. M. Wheeler et al., "How to design a dose-finding study using the continual reassessment method," *BMC Med. Res. Methodol.*, vol. 19, no. 1, p. 18, Jan. 2019, doi: 10.1186/s12874-018-0638-z.
- [94] S. M. Lee, N. A. Wages, K. A. Goodman, and A. C. Lockhart, "Designing Dose-Finding Phase I Clinical Trials: Top 10 Questions That Should Be Discussed With Your Statistician," *JCO Precis. Oncol.*, no. 5, pp. 317–324, Dec. 2021, doi: 10.1200/PO.20.00379.
- [95] S. Reagan-Shaw, M. Nihal, and N. Ahmad, "Dose translation from animal to human studies revisited," *FASEB J. Off. Publ. Fed. Am. Soc. Exp. Biol.*, vol. 22, no. 3, pp. 659–661, Mar. 2008, doi: 10.1096/fj.07-9574LSF.
- [96] B. Casadei and R. Wijesurendra, "Atrial fibrillation after cardiac surgery: to screen or not to screen?," *Cardiovasc. Res.*, vol. 117, no. 2, pp. e21–e23, Jan. 2021, doi: 10.1093/cvr/cvaa352.
- [97] J. A. Spertus, P. G. Jones, A. T. Sandhu, and S. V. Arnold, "Interpreting the Kansas City Cardiomyopathy Questionnaire in Clinical Trials and Clinical Care: JACC State-of-the-Art Review," *J. Am. Coll. Cardiol.*, vol. 76, no. 20, pp. 2379–2390, Nov. 2020, doi: 10.1016/j.jacc.2020.09.542.
- [98] S. Sheraz, H. Ayub, F. V. Ferraro, A. Razzaq, and A. N. Malik, "Clinically Meaningful Change in 6 Minute Walking Test and the Incremental Shuttle Walking Test following Coronary Artery Bypass Graft Surgery," *Int. J. Environ. Res. Public. Health*, vol. 19, no. 21, p. 14270, Nov. 2022, doi: 10.3390/ijerph192114270.
- [99] "Bicycle Stress Echocardiogram," Massachusetts General Hospital. Accessed: Nov. 20, 2023. [Online]. Available: <https://www.massgeneral.org/heart-center/treatments-and-services/bicycle-stress-echocardiogram>
- [100] "CR Scales | Sherry Grace." Accessed: Nov. 19, 2023. [Online]. Available: <https://sgrace.info.yorku.ca/cr-barriers-scale/>
- [101] N. Xiong et al., "Factors influencing cognitive function in patients with atrial fibrillation: a cross-sectional clinical study," *J. Int. Med. Res.*, vol. 47, no. 12, pp. 6041–6052, Dec. 2019, doi: 10.1177/0300060519882556.
- [102] "Value of Phase 1 Participant Recruitment -BioPharma Services." Accessed: Nov. 19, 2023. [Online]. Available: <https://www.biopharmaservices.com/blog/phase-1-recruitment-of-study-participants-is-vital-to-clinical-trials/>
- [103] Y. Masuda, H. D. Luo, G. S. Kang, K. L.-K. Teoh, and T. Kofidis, "Meta-analysis of the benefit of beta-blockers for the reduction of isolated atrial fibrillation incidence after cardiac surgery," *JTCVS Open*, vol. 3, pp. 66–85, Jul. 2020, doi: 10.1016/j.xjon.2020.07.004.
- [104] A. Goyal, P. Daneshpajouhnejad, M. F. Hashmi, and K. Bashir, "Acute Kidney Injury," in *StatPearls*, Treasure Island (FL): StatPearls Publishing, 2023. Accessed: Nov. 19, 2023. [Online]. Available: <http://www.ncbi.nlm.nih.gov/books/NBK441896/>
- [105] A. G. Zaman, R. A. Archbold, G. Helft, E. A. Paul, N. P. Curzen, and P. G. Mills, "Atrial Fibrillation After Coronary Artery Bypass Surgery," *Circulation*, vol. 101, no. 12, pp. 1403–1408, Mar. 2000, doi: 10.1161/01.CIR.101.12.1403.
- [106] "Secondary Prevention After Coronary Artery Bypass Graft Surgery | Circulation." Accessed: Nov. 19, 2023. [Online]. Available: <https://www.ahajournals.org/doi/10.1161/cir.0000000000000182>
- [107] S. Stavrakis et al., "Low-Level Transcutaneous Electrical Vagus Nerve Stimulation Suppresses Atrial Fibrillation," *J. Am. Coll. Cardiol.*, vol. 65, no. 9, pp. 867–875, Mar. 2015, doi: 10.1016/j.jacc.2014.12.026.
- [108] N. R. Mashayekhi, A. Alisaeeedi, A. Rostami, and P. Soltani, "The impact of colchicine in preventing postpericardiotomy syndrome; a double-blind clinical trial study," *Immunopathol. Persa*, vol. 6, no. 1, pp. e11–e11, Jan. 2020, doi: 10.15171/ipp.2020.11.
- [109] H. Kondo et al., "Splenectomy exacerbates atrial inflammatory fibrosis and vulnerability to atrial fibrillation induced by pressure overload in rats: Possible role of spleen-derived interleukin-10," *Heart Rhythm*, vol. 13, no. 1, pp. 241–250, Jan. 2016, doi: 10.1016/j.hrthm.2015.07.001.
- [110] moxi ltd, "Early treatment of atrial fibrillation for stroke prevention trial," Kofam. Accessed: Nov. 28, 2023. [Online]. Available: <https://kofam.ch/de/studienportal/nach-klinischen-versuchen-suchen/studie/28169>

- [111] L. A. Lopes and D. K. Agrawal, "Post-Operative Atrial Fibrillation: Current Treatments and Etiologies for a Persistent Surgical Complication," *J. Surg. Res.*, vol. 5, no. 1, pp. 159–172, 2022, doi: 10.26502/jsr.10020209.
- [112] B. J. Bachar and B. Manna, "Coronary Artery Bypass Graft," in *StatPearls*, Treasure Island (FL): StatPearls Publishing, 2023. Accessed: Nov. 19, 2023. [Online]. Available: <http://www.ncbi.nlm.nih.gov/books/NBK507836/>
- [113] G. H. Almassi et al., "New-onset postoperative atrial fibrillation impact on 5-year clinical outcomes and costs," *J. Thorac. Cardiovasc. Surg.*, vol. 161, no. 5, pp. 1803-1810.e3, May 2021, doi: 10.1016/j.jtcvs.2019.10.150.
- [114] D. T. Michaeli, J. C. Michaeli, T. Boch, and T. Michaeli, "Cost-Effectiveness of Lipid-Lowering Therapies for Cardiovascular Prevention in Germany," *Cardiovasc. Drugs Ther.*, vol. 37, no. 4, pp. 683–694, Aug. 2023, doi: 10.1007/s10557-021-07310-y.
- [115] D. Gotham, M. J. Barber, and A. M. Hill, "Estimation of cost-based prices for injectable medicines in the WHO Essential Medicines List," *BMJ Open*, vol. 9, no. 9, p. e027780, Sep. 2019, doi: 10.1136/bmjopen-2018-027780.
- [116] "R&D Costs," Knowledge Portal. Accessed: Nov. 19, 2023. [Online]. Available: <https://www.knowledgeportal.org/costs-r-d>
- [117] T. J. Moore, J. Heyward, G. Anderson, and G. C. Alexander, "Variation in the estimated costs of pivotal clinical benefit trials supporting the US approval of new therapeutic agents, 2015-2017: a cross-sectional study," *BMJ Open*, vol. 10, no. 6, p. e038863, Jun. 2020, doi: 10.1136/bmjopen-2020-038863.
- [118] A. Bessissow, J. Khan, P. J. Devereaux, J. Alvarez-Garcia, and P. Alonso-Coello, "Postoperative atrial fibrillation in non-cardiac and cardiac surgery: an overview," *J. Thromb. Haemost.*, vol. 13, pp. S304–S312, Jun. 2015, doi: 10.1111/jth.12974.
- [119] A. K. Ghose, V. N. Viswanadhan, and J. J. Wendoloski, "A knowledge-based approach in designing combinatorial or medicinal chemistry libraries for drug discovery. 1. A qualitative and quantitative characterization of known drug databases," *J. Comb. Chem.*, vol. 1, no. 1, pp. 55–68, Jan. 1999, doi: 10.1021/cc9800071.
- [120] C. A. Lipinski, F. Lombardo, B. W. Dominy, and P. J. Feeney, "Experimental and computational approaches to estimate solubility and permeability in drug discovery and development settings," *Adv. Drug Deliv. Rev.*, vol. 46, no. 1–3, pp. 3–26, Mar. 2001, doi: 10.1016/s0169-409x(00)00129-0.
- [121] "Veber's Rules in Terahertz Light." Accessed: Dec. 02, 2023. [Online]. Available: <https://www.researchsquare.com>
- [122] S. Park, Y.-H. Kim, H. I. Bang, and Y. Park, "Sample size calculation in clinical trial using R," *J. Minim. Invasive Surg.*, vol. 26, no. 1, pp. 9–18, Mar. 2023, doi: 10.7602/jmis.2023.26.1.9.

10. Supplementary Material

1) *In silico* screening:

Natural ligands	Molecule ID	PPAR target	PDB references
Omega-3 polyunsaturated fatty acids (PUFAs)	ITY	Alpha	https://www.rcsb.org/ligand/ITY
	EPA	Delta	https://www.rcsb.org/ligand/EPA

Table S1: Reference molecules of natural ligands, PPAR targets and corresponding PDB reference links.

Synthetic ligands from literature	Molecule ID	PPAR target	PDB references
Fibrates	PEM	Alpha, Delta and Gamma	https://www.rcsb.org/ligand/PEM
	BOG	Delta	https://www.rcsb.org/ligand/BOG
	F5A	Alpha	https://www.rcsb.org/ligand/F5A
	GW9	Alpha	https://www.rcsb.org/ligand/GW9
	P7F	Delta	https://www.rcsb.org/ligand/P7F
	GOL	Alpha and Delta	https://www.rcsb.org/ligand/GOL
	PLM	Alpha	https://www.rcsb.org/ligand/PLM
	2VN	Alpha	https://www.rcsb.org/ligand/2VN
	WY1	Alpha	https://www.rcsb.org/ligand/WY1
	T4T	Alpha	https://www.rcsb.org/ligand/T4T
	C5F	Alpha	https://www.rcsb.org/ligand/C5F
	EWR	Alpha	https://www.rcsb.org/ligand/EWR
	T02	Alpha	https://www.rcsb.org/ligand/T02
	T06	Alpha	https://www.rcsb.org/ligand/T06
	735	Alpha	https://www.rcsb.org/ligand/735
	Y1N	Alpha and Gamma	https://www.rcsb.org/ligand/Y1N
GW501516	7T1	Alpha and Delta	https://www.rcsb.org/ligand/7T1
	B7G	Delta	https://www.rcsb.org/ligand/B7G

Table S2: Reference molecules of synthetic ligands, PPAR targets and corresponding PDB reference links.

Dual-agonist ligand from literature	Molecule ID	PPAR target	PDB references
Elafibranor	BJB	Alpha, Delta and Gamma	https://www.rcsb.org/ligand/BJB
	KKB	Alpha, Delta and Gamma	https://www.rcsb.org/ligand/KKB
	MUO	Alpha and Delta	https://www.rcsb.org/ligand/MUO

Table S3: Reference molecules of dual-agonist synthetic ligands, PPAR targets and corresponding PDB reference links.

Property name	Minimal value	Maximal value	Weight in final score	Rules & References
Molecular weight	180	465	1	Ghose filter (160 <= MW <= 480) [119] & Lipinski's rule (MW <= 500) [120]
MolLogP	1	4.8	1	Ghose filter (-0.4 <= LogP <= 5.6) [119] & Lipinski's rule (LogP <= 5) [120]
Number of atoms (H excluded)	10	70	1	Ghose filter (20 <= #atom <= 70) [119]
Number of H-donors	0	4	1	Lipinski's rule (#donor <= 5) [120]
Number of H-acceptors	0	8	1	Lipinski's rule (#acceptor <= 10) [120]
Polar solvent accessible surface area	0	140	1	Veber's rule (<=140) [121]
Fraction of sp ³ -hybridized C (Fsp3)	0	0	0	Not very common
Volume	0	0	0	Not very common
Area	0	0	0	Not very common
Number of rotatable bonds	0	8	1	Veber's rule (<=10, optimally 7) [121]
Number of rings	1	6	1	Lepre et al (1 < #rings < 6) [30]
Number of aromatic rings	0	3	1	Lepre et al (#aromatic rings <=3)[30]

Table S4: Molecular constraints minimal and maximal values used in LEA3D tool.

In Table S4, we chose to set the weight in the final score as 1 for most of the properties to assign the same degree of importance. The weights of Fsp3, Volume and Area properties are set to 0 because they are not very commonly used. The last column shows some relevant references explaining the chosen respective values of each property.

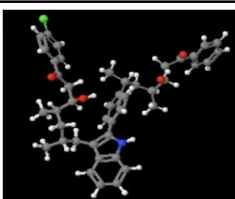
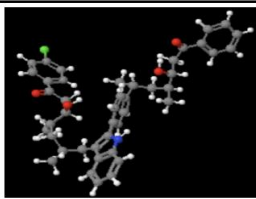
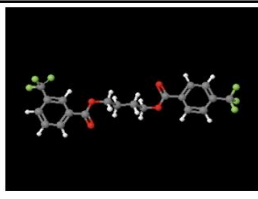
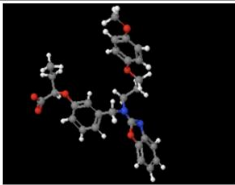
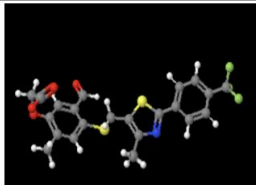
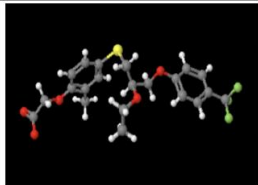
Dual-Agonist Compounds			
Without Constraints			
With Constraints			

Table S5: Dual-agonist ligands with the highest docking scores for PPAR α and PPAR δ .

2) In vivo validation:

PPAR α		Organ				
Species	Heart	Liver	Muscle	Brain	Kidney	
Mouse	69,81	94,7	78,92	57,17	90,31	
Rat	78,39	80,71	70,53	43,5	71,62	
Dog	78,32	79,07	85,44	47,73	66,53	
Pig	86,9	95,55	67,51	48,23	77,85	
Chimpanzee	73,36	68,13	75,37	44,39	62,95	
Sheep	66,56	81,6	75,81	55,89	90,38	
Human	87,81	92,09	81,77	71,02	70,21	
Göttingen mini pig						

PPAR δ		Organ				
Species	Heart	Liver	Muscle	Brain	Kidney	
Mouse	10,019	4,256		5,195	9,943	
Rat	0,944	0,13	0,405	0,208	0,449	
Dog						
Pig	4,899	3,438	4,161		8,361	
Chimpanzee						
Human	3,913	1,35		7,428	3,554	
Göttingen mini pig						
Sheep						

Table S6: Expression profiles of PPAR α and PPAR δ using respectively Bgee databases NCBI databases [59], [60].

For PPAR α , the values obtained are the expression scores going from 0 to 100 while for PPAR δ , the values obtained are the Reads Per Kilobase per Million mapped reads (RPKM).

3) Clinical Trials:

The number of individuals for **Phase I** is calculated as follows: 4 cohorts of 3 individuals each ($4 \times 3 = 12$) plus another 12 in case there are subjects showing side effects (24 in total). Other 12 patients will be used for the second escalation study (36 in total).

The number of individuals for **Phase II** is calculated assuming a medium effect size of $d = 0.7$, a power = 0.8 (standard in statistics) and an $\alpha = 0.01$ (also standard). The effect size was chosen based on a different paper as explained in the clinical trials. A power of 0.8 means that the study is optimally equipped to detect meaningful effects, with an 80% probability of accurately identifying real changes (i.e. between the placebo and the treatment).

Considering we will use 4 cohorts and each cohort has a sample size of 50, obtained using the parameters mentioned before, the total sample size is $50 \times 4 = 200$.

The number of individuals for **Phase III** is calculated as previously, but with 2 cohorts, each of 262 subjects.

A two-sample t-test will be implemented; although it may be considered somewhat simplistic, it provides a first indication of the number of individuals needed for phases 2 and 3 of the clinical trials.

Code used in R for phases 2 and 3 [122]:

```
library(pwr)
effect_size <- 0.7
alpha <- 0.01
power <- 0.8
sample_size_cohort <- pwr.t.test(d = effect_size, sig.level = alpha, power = power, type = "two.sample")
sample_size_cohort
```